Original article

MOLECULAR METABOLISM

Essential role of germ cell glycerol-3-phosphate phosphatase for sperm health, oxidative stress control and male fertility in mice

Abel Oppong[1,9], Yat Hei Leung[1,9], Anindya Ghosh[1], Marie-Line Peyot[1], Marilène Paquet[2], Carlos Morales[3], Hugh J. Clarke[4], Fahd Al-Mulla[5], Alexandre Boyer[2], S. R. Murthy Madiraju[1], Derek Boerboom[2], Cristian O'Flaherty[3,6,7,8,], Marc Prentki[1,*]**

ABSTRACT

Objectives: Obesity, diabetes and high-calorie diets are associated with defective sperm function and lowered male fertility. Mature spermatozoa primarily use fructose and glucose, and glucose and glycerol metabolism are important for sperm function. We recently discovered a novel mammalian enzyme, glycerol-3-phosphate (Gro3P) phosphatase (G3PP), and showed that it operates the glycerol shunt by hydrolyzing Gro3P to glycerol, and regulates glucose, lipid and energy metabolism in pancreatic β-cells and liver. We now observed that G3PP expression is the highest in the testis and spermatozoa, and investigated its role in male fertility.

Methods: We examined G3PP expression during spermatogenesis in mouse and assessed male fertility and spermatozoon function in conditional germ cell specific G3PP-KO (cG3PP-KO) mice and tamoxifen-inducible conditional germ cell G3PP-KO (icG3PP-KO) mice. We also determined the structural and metabolic parameters and oxidative stress in the spermatozoa from icG3PP-KO and control mice.

Results: G3PP expression in mouse spermatocytes and spermatids markedly increases during spermatogenesis. Male cG3PP-KO mice, in which germ cell G3PP is deleted from embryonic stage, are infertile due to dysfunctional sperm with reduced motility and capacitation, and elevated spontaneous acrosomal reaction and oxidative stress. However, icG3PP-KO male mice do not have altered fertility, due to the presence of ∼10% normal spermatozoa. icG3PP-KO spermatozoa display significantly reduced functionality and morphological and ultrastructural alterations. The icG3PP-KO spermatozoa show reduced glycerol production, elevated levels of Gro3P and reactive oxygen species (ROS), and oxidative stress that is associated with increased mitochondrial membrane potential.

Conclusions: Germ cell G3PP deletion leads to the generation of spermatozoa that are functionally and structurally abnormal, likely due to the build-up of Gro3P that increases mitochondrial membrane potential, ROS, and oxidative stress and alters spermatozoa function. Overall, the results indicate that G3PP and the glycerol shunt are essential for normal spermatozoa function and male fertility.

Keywords Glycerol-3-phosphate; Glycerol-3-phosphate phosphatase; G3PP; Glycerol shunt; Male fertility; ROS; Mitochondria; Oxidative stress

1. INTRODUCTION

A declining trend is seen worldwide in male reproductive health [1] and this is ascribed to reduced spermatogenesis, altered sperm morphology, mobility, and function, likely due to genetic, environmental and lifestyle factors [2]. The increasingly prevalent conditions of obesity and type 2 diabetes (T2D) and diets rich in calories are often accompanied by lowered male fertility [3,4]. Indeed, excess glucose concentration in the storage media has been shown to have toxic effects on stallion spermatozoa, which could be prevented by low glucose levels together with supplementation of Krebs cycle substrates [5,6]. Mature human spermatozoa primarily use fructose and glucose as energy sources and conduct high rates of glycolysis, which occurs in the principal piece, whereas mitochondrial ATP production is restricted to the midpiece. The energy source for the acrosome reaction is not known [7].

There is evidence that disturbed glycerol metabolism in sperm cells contributes to sperm alterations and male infertility [8]. Disturbed

[1]Departments of Nutrition, Biochemistry and Molecular Medicine, University of Montreal, and Montreal Diabetes Research Center, Centre de Recherche du Centre Hospitalier de l'Université de Montréal (CRCHUM), Montréal, QC, Canada [2]Centre de recherche en reproduction et fertilité (CRRF), Université de Montréal, Saint-Hyacinthe, Québec, Canada [3]Anatomy and Cell Biology, Faculty of Medicine and Health Sciences, McGill University, Montréal, Québec, Canada [4]Departments of Obstetrics and Gynecology and Biology, Division of Experimental Medicine, McGill University, Montréal, Canada [5]Translational Medicine Department, Dasman Diabetes Institute, Kuwait [6]Surgery (Urology Division), Faculty of Medicine and Health Sciences, McGill University, Montréal, Québec, Canada [7]Pharmacology and Therapeutics, Faculty of Medicine and Health Sciences, McGill University, Montréal, Québec, Canada [8]The Research Institute, McGill University Health Centre, Montréal, Québec, Canada

[9] Abel Oppong and Yat Hei Leung contributed equally to this work

*Corresponding author. CRCHUM, Viger Tower, 900 Saint Denis St, R-08-436, Montréal, QC H2X 0A9, Canada. E-mail: marc.prentki@umontreal.ca (M. Prentki).

**Corresponding author. The Research Institute, McGill University Health Centre, Montréal, QC H4A 3J1, Canada. E-mail: cristian.oflaherty@mcgill.ca (C. O'Flaherty).

Received September 12, 2024 • Revision received October 30, 2024 • Accepted November 5, 2024 • Available online 13 November 2024

https://doi.org/10.1016/j.molmet.2024.102063

glucose and lipid metabolism in obesity and T2D leads to elevated glycerol levels in tissues and blood, and excessive extracellular glycerol levels in the testis negatively impact spermatogenesis [9]. However, under physiological conditions, glycerol plays an essential role in maintaining sperm cell volume [10,11]. Considering that post-testicular spermatozoa face continuously changing extracellular osmotic conditions that range from an osmolality of 480 mmol/kg in the corpus epididymis to 294 mmol/kg in seminal fluid following ejaculation and to 268–284 mmol/kg in the cervical mucus, the necessity of sperm cell volume regulation becomes evident [11]. The organic osmolyte property of glycerol is dependent on its transmembrane transport through aquaglyceroporins (AQP) and defects in AQPs cause disrupted sperm volume regulation and male infertility in mice and humans [10–14].

Glucose-derived glycerol in mammalian cells was thought to be produced only through the esterification of glycerol-3-phosphate (Gro3P) to fatty acids to produce triglycerides (TG), followed by lipolysis by adipose triglyceride lipase (ATGL), hormone-sensitive lipase (HSL) and monoacylglycerol lipase (MAGL), which hydrolyze TG, diacylglycerol and monoacylglycerol, respectively [15,16]. In addition to MAGL, we recently showed that α,β-hydrolase domain containing-6 (ABHD6), a membrane-bound enzyme, also hydrolyzes monoacylglycerol [17]. However, lipolysis is not the only source of glycolysis-derived glycerol, as we recently identified a Gro3P phosphatase (G3PP) in mammalian cells that can hydrolyze Gro3P to glycerol [18]. G3PP is an ubiquitous enzyme but by far, its highest expression of all tissues in mice is in the testis [18], suggesting the possibility that G3PP plays an essential role in this organ or sperm cells themselves [18]. Our recent work showed that G3PP controls glucose, lipid, and energy metabolism in pancreatic β-cells [19] and liver [20], particularly under hyperglycemic conditions, and is a stress-induced enzyme in *C. elegans* [21,22]. Thus, the evidence emerges that G3PP acts as a glucose excess detoxification machine as glucose-derived glycerol is a relatively inert molecule, whereas elevated glucose is quite toxic [23,24]. In *C.elegans,* where we identified three G3PP/PGPH homologs, increased G3PP expression was found to counteract many stresses (osmotic, cold, oxidative, glucotoxicity), and it also increases lifespan and promotes healthy aging [19–22]. Thus, G3PP is the key component of a novel metabolic pathways that we have termed the "glycerol shunt" in which glycolysis-derived dihydroxyacetone phosphate (DHAP) is transformed to Gro3P via Gro3P dehydrogenase-1 (GPD1), then Gro3P to glycerol via G3PP, and finally glycerol escapes cells via AQPs. Indeed, this pathway shunts glucose- or fructose-derived carbons away from lactate production, the Gro3P shuttle, mitochondrial metabolism and TG synthesis [20,23]. The G3PP protein is encoded by the *PGP* gene and certain forms of male infertility in humans, such as teratozoospermia, are associated with mutations in this gene [25]. Moreover, patients with nonobstructive azoospermia were found to have reduced expression of the *PGP*/G3PP gene in the testis, compared to normal controls [26]. In addition, a recent study on testicular seminoma patients with reduced fertility identified G3PP expression to be reduced by ~50-fold in the seminoma sperm, compared to healthy controls, even though the relation between G3PP expression and spermatozoa function is not known [27]. On the other hand, male mice with a lack of either the lipolysis enzymes ATGL [28] or HSL [29] that contribute to lipolysis-derived glycerol are infertile, whereas male mice with deletion of either MAGL [30] or ABHD6 [17], the enzymes that actually produce glycerol, are fertile. Perhaps the redundance of MAGL and ABHD6 may explain why each of these KO mice are fertile. The available database information (Human Protein Atlas) indicates that the expression of ATGL, HSL and MAGL proteins in the spermatozoa is very low, whereas G3PP is very high, implying that the contribution of lipolysis for glycerol release in the sperm cells is much less than that via the glycerol shunt. Moreover, spermatozoa utilize Gro3P that is produced from fructose, glucose or phospholipid metabolism [8]. GPD2 oxidizes Gro3P to DHAP [31–33], a step that can lead to the production of reactive oxygen species (ROS) [8], which can cause male infertility when excessively produced [34]. It has been shown earlier that stallion spermatozoa stored in media with excess glucose undergo ferroptosis due to the formation of elevated levels of ROS [5] and also suffer from structural damage due to the production of glycating compounds such as methylglyoxal, during glycolysis [6]. Thus, the action of G3PP to control the levels of Gro3P is possibly important to prevent excess production of ROS in spermatozoa, and this has never been investigated. Hence, it can be hypothesized that G3PP/PGP and the glycerol shunt are essential for sperm function and male fertility.

Here, we address the role of this novel enzyme and metabolic pathway, G3PP and the glycerol shunt, in the regulation of sperm intermediary metabolism and function. Mouse models with both conditional and inducible conditional G3PP/PGP knockout in the male germinal cells were used. We demonstrate that G3PP expression markedly rises during sperm cell differentiation and is essential for sperm cell function and male fertility. Spermatozoa with G3PP deletion are defective in their morphology and function. These spermatozoa show elevated Gro3P and reduced glycerol production, relatively minor alterations in the level of many metabolites, but altered mitochondrial membrane potential and a high degree of oxidative stress.

2. MATERIALS AND METHODS

2.1. Experimental animals

All animal procedures were approved by the Comité d'éthique de l'utilisation des animaux (CÉUA — institutional animal care and use committee; Protocol # Rech-2053) of the Faculté de médecine vétérinaire of the Université de Montréal and by the CRCHUM animal ethics committee (Protocol # CM19035MPs) and conformed to the International Guiding Principles for Biomedical Research Involving Animals. Mice were housed in microisolator cages, 12h light/dark cycle, and fed ad libitum (Rodent Chow 5075 from Charles River Laboratories; Wilmington, MA, USA). The C57BL/6N strain mice were obtained from Charles River Laboratories. Transgenic Vasa-Cre [(Ddx4-cre)1Dcas/J; Strain # 006954] and Vasa-Cre^{ERT2} [(Ddx4-cre/ERT2)1Dcas/J; Strain # 024 760] mice were obtained from Jackson Laboratory (Bar Harbor, ME, USA). G3PP-floxed (G3PP$^{flox/flox}$) mice were described before [19]. We initially generated conditional, germ cell-specific G3PP-KO mice by mating G3PP$^{flox/flox}$ mice [19] to Cre expressing transgenic mice in which Cre expression is driven by the *Ddx4* promoter (JAX #006954) [35]. G3PP$^{flox/-}$;Vasa-Cre mice (cG3PP-KO) were generated by mating female G3PP$^{flox/flox}$ mice to G3PP$^{flox/+}$;Vasa-Cre males. The latter mice were only used for breeding until 9 weeks of age in order to minimize Cre activity in the sperm, and hence the odds of global recombination occurring in the embryo. Nonetheless, cG3PP-KO mice were born in numbers ≈20-fold lower than the expected Mendelian ratio, suggesting high levels of gene inactivation in the embryo and embryonic lethality. Because of this, we could not obtain sufficient number of male cG3PP-KO mice to conduct all the studies. In order to circumvent this problem, we next generated tamoxifen-inducible conditional germ cell G3PP-KO mice (icG3PP-KO). These icG3PP-KO mice were generated by breeding Vasa-Cre^{ERT2} [36] mice with G3PP$^{flox/flox}$ mice for several generations to obtain G3PP$^{flox/flox}$;Vasa-Cre/ERT2 mice. To inactivate G3PP in male germ cells in the inducible model, 6-8week-old G3PP$^{flox/flox}$;Vasa-Cre/ERT2 mice were injected with tamoxifen

(120 mg/kg, IP) in corn oil or vehicle alone once daily for 5 consecutive days. After an eight weeks period, to allow for a complete cycle of spermatogenesis and transit through the epididymis, the animals were used in experiments. The production of G3PP$^{flox/flox}$;Vasa-Cre/ERT2 mice followed Mendelian ratio and mice were in sufficient numbers, to be used in most experiments. Both the Vasa-Cre and Vasa-CreERT2 mice were on C57BL/6J genetic background whereas the G3PPflox/flox mice were on pure C57BL/6N genetic background and thus the resulting KO mice were on a mixed NJ background. As we compared the KO mice to Cre, flox and WT controls that gave similar results and all these control mice breed normally, we do not see a problem that the KO mice were on the NJ background.

2.2. Fertility analysis

Fertility in the cG3PP KO model was assessed by mating 8-week old male G3PP$^{flox/flox}$ (controls) and male cG3PP-KO mice (n = 3 for each genotype) with 8-week-old female C57BL/6J WT mice for a period of 3 months and counting the number of litters and pups produced. In the icG3PP-KO model, fertility was assessed by mating 16-week-old icG3PP-KO (n = 6, G3PP$^{flox/-}$;Vasa-Cre/ERT2-TMX) and control (n = 4, G3PP$^{flox/flox}$;Vasa-Cre/ERT2-Vehicle) males with 8 week-old WT females for a period of 6 months, and counting the number of litters and pups produced. Males were removed after 6 months and females were monitored for three weeks for the production of a final litter.

2.3. In vivo fertilization

Eight-week-old female WT mice (n = 3) were superovulated by injecting intraperitoneally with 7.5 IU Folligon PMSG (Pregnant Mare Serum Gonadotrophin; Merck, NJ), followed by an injection of 5 IU Chorulon (human Chorionic Gonadotropin; Merck, NJ) 48 h later. These female mice were placed individually in cages with either a single cG3PP-KO male mouse or a WT male mouse (both 8 weeks of age). Vaginal plugs were checked the next morning to confirm mating. The females were sacrificed at 18 h after hCG injection, their oviducts were removed, and the egg masses were collected and incubated for 10 min in a pre-warmed solution of hyaluronidase (10 μg/ml, Sigma Chemicals, USA) in HEPES-buffered minimal essential medium, pH 7.2 (Invitrogen, USA) to disaggregate the cells. All the eggs were fixed in a solution of 2% (w/v) paraformaldehyde in PBS for 10 min on glass slides, then in blocking buffer (PBS, 0.3% bovine serum albumin, 0.1% Triton X-100). The prepared slides were stained with 4,6-diamidino-2-phenylindole (DAPI) and analyzed under a fluorescent microscope and eggs with two pronuclei were counted as fertilized eggs and the rate of fertilization was calculated as the percentage of cleaved embryos of the total recovered embryos/eggs [37,38].

2.4. Sperm sample collection

Sperm were collected from the cauda epididymis as described before [39] in non-capacitation Biggers, Whitten and Whittingham (ncBWW) medium consisting of 112 mM NaCl, 4.6 mM KCl, 1.2 mM $MgSO_4$, 1.2 mM KH_2PO_4, 1.7 mM $CaCl_2$, 20 mM HEPES (pH 7.4), 5.6 mM glucose, 1 mg/ml fatty acid-free BSA, 2 mM $NaHCO_3$, 0.27 mM sodium pyruvate, and 21.6 mM sodium lactate. Testes and epididymides were isolated and separated using a previously described protocol [39] with few modifications. Fat was trimmed from testes and epididymides in PBS and the entire epididymides were then transferred to 60 mm Petri Dishes containing ncBWW medium, after which the caudal portion was separated and transferred to 35 mm dishes containing 1 ml of ncBWW medium. Spermatozoa were released into the medium by nicking the cauda open, followed by incubation at 37°C for the spermatozoa to swim out. The sperm suspensions were collected in 1.5 ml microfuge tubes and spermatozoa counts were obtained by 10-fold dilution in PBS followed by incubation at 60°C for 2 min for heat shock prior to counting using a hemacytometer.

2.5. Glycerol release

Glycerol released from caudal spermatozoa was measured in two independent experiments, each with spermatozoa pooled from 3 to 5 mice from each genotype. Spermatozoa from multiple icG3PP-KO and TMX treated G3PP$^{flox/flox}$ -control mice were pooled respectively in 15 ml falcon tubes, following swim-out in the modified ncBWW medium without sodium pyruvate and sodium lactate, for 30 min at 37°C as described above. Sperm samples were centrifuged at 900×*g* for 2 min, and the supernatant was removed. The pooled sperm pellets for each genotype were then resuspended in 2.5 ml of the ncBWW medium. Aliquots of sperm suspension (0.5 ml) were added to 12-well plates containing 0.5 ml of ncBWW medium containing 5.6 mM glucose with and without 5 mM fructose or 25 mM glucose at 37°C. Aliquots were taken from the wells immediately after adding the samples (t = 0) and after 1-hour incubation (t = 60 min), and centrifuged at 900×*g* for 2 min. Supernatants were collected for glycerol assay [18]. In both the experiments, glycerol measurements were made in duplicate, and normalized to sperm counts.

2.6. Metabolomics

Spermatozoa isolated from cauda epididymis from control and icG3PP-KO mice were isolated in 1 ml of ncBWW medium. After obtaining sperm counts, the remaining sperm suspensions were centrifuged at 900×*g* for 2 min, and the supernatant was aspirated until about 60 μl remained. Then, 600 μl of extraction buffer, consisting of methanol and ammonium acetate, was added to the pellets to reach 80% v/v methanol and 2 mM ammonium acetate (pH 9.0). After mixing for 10 s, the samples were left on ice for 15 min. Then, the samples were homogenized by sonication in a cup horn at 150W with pulse cycles of 10 s on and 10 s off, followed by centrifugation at 20 000×*g* for 10 min at 4°C. The supernatant (600 μl) was transferred to glass tubes and liquid/liquid extraction was performed by adding 168 μl of water and 960 μl of 3:1 chloroform:heptane and after cooling on ice for 10 min, the tubes were centrifuged at 4,500×*g* for 15 min at 4°C. Approximately 550 μl of the upper aqueous phase was transferred to 1.5 ml screw cap tubes, which were placed in a Centrivap Concentrator (Labconco, MO) at 25°C for at least 90 min to remove methanol, followed by freezing in liquid N_2 for 1 min, and lyophilization to dryness. The residue was suspended in 20 μl water and after centrifugation for 5 min at 4°C, 16 μl of the supernatant was processed for LC-MS/MS. All the measured metabolites were normalized to sperm counts from the corresponding mice.

2.7. Mitochondrial membrane potential

Caudal spermatozoa from icG3PP-KO and control mice were isolated in 1.7 ml of non-capacitation BWW medium with a swim-out incubation of 30 min at 37°C. The sperm suspensions were split into three 500 μl aliquots in 1.5 ml microfuge tubes. Then 10 μl of JC-1 reconstituted reagent (MitoProbe JC-1 Assay kit; Thermo Fisher Scientific, MA) was added, and the tubes were incubated for 30 min at 37°C. These tubes were centrifuged at 900×*g* for 2 min, and the sperm pellets were washed twice with 1 ml of PBS by centrifugation at 900×*g* for 2 min. Sperm pellets were resuspended in 500 μl of PBS, and fluorescence was analyzed at excitation (λ = 488 nm) and emission (λ = 525 nm) wavelengths, in duplicate, on a LSR Fortessa X-20 fluorescence-activated cell sorter (BD, NJ). The data were further analyzed using FlowJo software v10.7.0 (FlowJo, LLC).

2.8. ROS production

Caudal sperm (500 μl aliquots) in 1.5 ml tubes was mixed with a methanolic solution of 2′,7′—dichlorofluorescin diacetate (DCFDA) (Sigma Aldrich, MO) to obtain a final concentration of 10 μM. Samples were incubated for 30 min at 37°C and washed twice by resuspension in 1 ml PBS and centrifugation at 900×*g* for 2 min. The sperm pellets were resuspended in 300 μl PBS and fluorescence was measured at excitation (488 nm) and emission (525 nm) wavelengths on a LSR Fortessa X-20 flowcytometer (BD, NJ), and the data were analyzed using FlowJo software v10.7.0 (FlowJo, LLC).

2.9. Immunohistochemistry

Testes and epididymides were isolated and fixed in 10% Bouin's solution for 24h, washed three times in 70% ethanol (24h per wash) and embedded in paraffin blocks. Following sectioning (3 μm), deparaffinization, rehydration, and antigen retrieval were performed using either sodium citrate heat-treatment or using trypsin (1:3 ratio in PBS for 15 min at 37°C), and then the tissue sections were incubated with anti-G3PP primary antibody (1:400 dilution; sc-390883; Santa Cruz Biotechnology, TX) overnight at 4°C. Detection was performed using the standard avidin—biotin—peroxidase complex method with either the Vectastain Elite ABC HRP Kit followed by the DAB Peroxidase (HRP) Substrate Kit (Vector Laboratories, CA), or the HRP/DAB Detection IHC Kit (Abcam, UK) according to the manufacturer's instructions. Slides were counterstained with hematoxylin prior to mounting.

2.10. Western blot

Proteins from the cG3PP-KO and control mice testes were extracted using T-PER tissue protein extraction reagent (Thermo Scientific, MA) to examine the expression of G3PP protein. Proteins from tissues and spermatozoa from the icG3PP-KO and different control mice were extracted in RIPA lysis buffer (150 mM NaCl, 50 mM Tris base pH 8.0, 1% Triton X-100, 0.5% sodium deoxycholate and 0.1% SDS) supplemented with a cocktail of protease inhibitors (aprotonin, leupeptin, pepstatin and phenylmethylsulfonyl fluoride). All lysates were sonicated and the total protein was quantified. Proteins were resolved on 10% SDS-polyacrylamide gels and processed for immunoblotting [19]. Membranes were blocked with 5% non-fat dry milk in TBST (Tris-buffered saline supplemented with 0.1% Tween 20 (BioShop, ON)) and probed with anti-G3PP antibody (1:1000 dilution; sc-390883; Santa Cruz Biotechnology, TX) overnight at 4°C followed by incubation for 1 h at room temperature with either anti-rabbit IgG HRP Conjugate (1:10 000 dilution; W4011; Promega, WI) or anti-mouse IgGK BP-HRP (1:10 000 dilution; sc-516102; Santa Cruz Biotechnology, TX). Antibodies to detect α-tubulin, β-actin, and GAPDH (loading controls) were prepared in TBST with 5% non-fat milk as follows: α-tubulin (1:10 000 dilution; ab4074; Abcam, UK) with 30 min incubation at room temperature; β-actin (1:10 000 dilution; Sigma Chemicals; A5441; MO) with 30 min incubation at room temperature; and GAPDH (1:1000 dilution; #2118; Cell Signaling, MA) with overnight incubation at 4°C. Luminescent signal was generated using Immobilon Western Chemiluminescent HRP substrate (MilliporeSigma, MA) and quantified. Expression of G3PP protein in the samples was normalized to the loading controls.

2.11. Sperm motility

Sperm motility was determined as done before [40]. In brief, spermatozoa were collected from cauda epididymides in PBS (pH 7.4) after a swim-out incubation for 10 min at 37°C. Then, the sperm aliquot was supplemented with 5 mg/ml BSA and sperm cell number was adjusted to determine total and progressive sperm motility using a computer-assisted sperm analysis (CASA) system with Sperm Vision HR software version 1.01 (Minitube, Canada), as described before [40].

2.12. Sperm capacitation

The spermatozoon must undergo a series of biochemical and morphological changes, collectively called sperm capacitation, in order to recognize the oocyte, induce the acrosome reaction, and achieve fertilization. Sperm samples were incubated in BWW medium with or without capacitation inducers (5 mg/ml BSA + 25 mM HCO_3) for 60 min at 37°C. Then the samples were centrifuged at 600×*g* for 5 min at 20°C. The supernatant was discarded, and the sperm pellets were resuspended in fresh BWW medium and incubated with 10 μM progesterone for 30 min at 37°C to promote the acrosome reaction [41,42]. All Incubations were at 37°C in 5% CO_2 incubator. Sperm samples were then fixed with 4% paraformaldehyde for 15 min at 20°C, centrifuged at 350×*g* for 5 min, and the pellets were resuspended in BWW medium. The fixed sperm samples were smeared onto Superfrost slides, air dried, and incubated with 1:10 diluted Giemsa stain for 90 min. After washing, the slides were processed to assess the percentage of spermatozoa with intact and reacted acrosomes in 200 spermatozoa per sample using a Leica DM500 microscope (Opti-Tech Scientific, QC) at 600 × magnification. The percentage of acrosome reaction (AR) was defined as the percentage of Giemsa stain-negative spermatozoa. Spontaneous AR (SAR) was defined as the percentage of Giemsa stain-negative spermatozoa at zero time. The actual progesterone-stimulated % AR was obtained by subtracting the % SAR from the total observed % AR in non-capacitated and capacitated spermatozoa. The percentage of sperm capacitation was defined as the % AR obtained by subtracting the % AR in capacitated spermatozoa from the % AR in non-capacitated spermatozoa [41,42].

2.13. Oxidative stress

Lipid peroxidation: Oxidative stress in the spermatozoa was assessed by measuring the levels of 4-hydroxynonenal (4-HNE), a product of lipid peroxidation, and DNA oxidation by measuring 8-hydroxy deoxyguanosine (8OHdG). The levels of 4-HNE in sperm plasma membrane were determined by smearing non-permeabilized sperm samples [43] onto Superfrost slides, followed by drying at 37°C. Samples were rehydrated with PBS + Triton 0.1% (PBS-T) for 5 min, and incubated for 30 min at 37°C in horse serum (1%) in PBS-T to block nonspecific antibody binding. Slides were washed with PBS-T and incubated overnight at 4°C with the goat polyclonal anti-4-HNE antibody (Abcam, Canada) diluted in 1% horse serum in PBS-T. Then, the slides were washed and incubated with 1:2000 diluted donkey anti-goat secondary antibody conjugated with AlexaFluor 555 (ThermoFisher, Canada) for 1 h at 37°C. The slides were rewashed, and ProLong Antifade with DAPI (Molecular Probes, USA) was added before the coverslips were placed. The negative control was incubated with secondary antibody alone. ImageJ was used for quantification of the average relative fluorescence intensity (RFI) of at least 200 spermatozoa per sample.

Sperm DNA oxidation: Formation of 8OHdG was determined as before [41,43]. In brief, sperm samples were smeared onto Superfrost slides and air-dried and were treated with 50 mM Tris—HCl, pH 7.4 buffer, containing 1% SDS, 40 mM DTT and 1 mM EDTA for 5 min. Then the slides were washed with PBS and incubated with 5% goat serum in PBS-T for 1 h at 37°C. After washes in PBS, the slides were incubated with anti-8OHdG antibody (1:100 diluted in 1% goat serum in PBS-T; StressMarq, Canada) overnight at 4°C. After incubation, the slides

were washed and incubated with goat anti-mouse secondary antibody conjugated with AlexaFluor 555 (1:2000 diluted in PBS-T plus 1% BSA; ThermoFisher, Canada) for 1 h at 37°C. Finally, the slides were rewashed, and ProLong Antifade with DAPI (Molecular Probes, USA) was applied and covered with coverslips. Negative control was set up by incubation without the primary antibody. The specificity of the anti-8OHdG antibody was ascertained as before [44]. Imaging and quantifying were as described above. Results of DNA oxidation were expressed as percentages of spermatozoa with a strong signal for 8-OHdG (>10RFI).

2.14. Morphological examination of spermatozoa by light and electron microscopy

Light microscopy was done on the freshly isolated spermatozoa to assess morphological integrity and abnormalities. Abnormal spermatozoa included the sperm with head abnormalities: amorphous head, absence of head, big head, small head, round head, and absence of acrosome; midpiece abnormalities: thin midpiece and midpiece bent at different degrees; and tail abnormalities: no flagellum, more than one flagellum, curly tail or folded tail (different degrees), and short tail. Transmission electron microscopy (TEM) was conducted to assess structural defects after fixing the caudal spermatozoa in 2.5% glutaraldehyde in 0.1 M sodium cacodylate buffer, pH 7.4 overnight. Then, samples were centrifuged at 200×*g* for 2 min and washed twice with PBS. Sperm pellets were then embedded in 2% low melting agarose solution in water that was pre-heated to 37°C. After cooling to 4°C, the agarose blocks were cut with a diamond knife, mounted on copper grids and stained for 5 min with uranyl acetate followed by a 3 min incubation in lead citrate. The copper grids with mounted samples were examined with a FEI Tecnai 12 120 kV Transmission Electron Microscope (Nanoimaging Services, USA).

3. RESULTS

3.1. Expression of G3PP in the testis, epididymis and spermatozoa

We earlier reported that testis has markedly high expression of G3PP [18]. The present results confirm the high level of G3PP protein expression in the whole testis compared to other tissues of mouse, and the expression in mature spermatozoa collected from cauda epididymis was found to be 30-fold higher than in most tissues, besides testis, when the expression is normalized to β-actin or GAPDH (Figure 1A), which suggests a particularly important and overlooked role of G3PP and the glycerol shunt in sperm function and health.

In order to better understand the role of G3PP in male reproduction, we first examined G3PP expression in the seminiferous epithelium during different stages of spermatogenesis (Figure 1B). G3PP protein is not detectable in the mouse spermatogonia through all stages. In spermatocytes, cytoplasmic expression varies from mild in stages I and VI-VII to moderate in stages II-III. There was strong G3PP staining in round and elongating spermatids, in the cytoplasm and also in the nucleus and the G3PP staining appeared to be strongest at the spermiation stage, but this could be due to the contraction of the cytoplasm (Figure 1B). It has been reported in a database that during spermatogenesis in humans (http://bio-add.org:6688/SperMD/show?id=SMDBT013452), expression of the *PGP* gene increases steadily from spermatogonia to spermatocytes and reaches maximal expression in round and elongated spermatids and mature sperm [45,46]. In the epididymis, where maturation of spermatozoa occurs, relatively weak G3PP expression was seen in the cilia of the efferent ductules and in the cytoplasm and stereocilia of the principal cells (Figure 1C). However, relatively much higher expression of G3PP was noticed in the corpus epithelium. The expression of G3PP is relatively low in the caput of the epididymis, increases to a strong expression in the corpus segment and decreases to a weak expression in the cauda (tail) segment and vas deferens. (Figure 1C).

3.2. Conditional and inducible-conditional deletion of G3PP in embryonic germ cells

We generated mice with both conditional or tamoxifen-inducible conditional G3PP knockout in the germ cells. Deletion of G3PP protein, after normalization to either α-tubulin or β-actin was confirmed by Western blot analysis in the testis lysates in cG3PP-KO mice (Figure 2A) and icG3PP-KO mice (Figure 2B) and also in the sperm isolated from control and icG3PP-KO mice (Figure 2C). Immunohistochemistry of the testis from the WT, $G3PP^{flox/flox}$ and cG3PP-KO confirmed the complete deletion of G3PP in the germ cells of the KO mice (Figure 2D). Similarly, G3PP protein deletion was confirmed in the testis sections of icG3PP-KO mice (at 40 × , 200 × and 600 × magnification) as compared to the Flox-TMX control mice (Figure 2E). However, in the icG3PP-KO mouse testis, a small number of tubules with G3PP expression could be noticed, indicating a heterogeneous/mosaic and incomplete recombination. This also explains the presence of very low levels of G3PP detected by Western blot analysis in the icG3PP-KO sperm (Figure 2C).

3.3. Male cG3PP-KO mice are infertile

As mentioned above, cG3PP-KO mice were born in numbers ≈20-fold lower than the expected Mendelian ratio, indicating significant embryonic lethality. In the Vasa-cre mouse model used here, the Vasa promoter directed Cre expression to male germ cells has both the desired and also some undesired effects, at the same time. The undesired effect occurs because when the sperm cell expressing Cre enzyme fertilizes the G3PP-floxed oocyte, this causes the floxed alleles (G3PP/*PGP*) to recombine shortly after fertilization, giving rise to a G3PP-knockout embryo, that is nonviable beyond E11.5 [47]. We could manage to get a few cG3PP-KO mice as we used very young (6–9 wk old) Vasa-cre males for breeding, and at that young age the sperm produced by the Vasa-cre males contains relatively little Cre (reasons unknown), thereby avoiding the recombination and gene deletion when the sperm meets the egg. However, despite using the young Vasa-cre males, we got a very high level of embryonic lethality, and much fewer cG3PP-KO offspiring than anticipated. Even though we have not determined the time course of G3PP deletion, the conditional deletion of G3PP likely starts in the embryos at E15-E18 in the male germ cells when the Cre expression and activity are detected, as reported before in the transgenic Vasa-Cre (Ddx4-cre) mouse model [35]. The Cre-mediated G3PP knockout is expected to reach 90–95% around day 5 after birth, on the basis of earlier reported Cre-mediated recombination in male germ cells [35]. We examined the ability of male cG3PP-KO or icG3PP-KO mice to breed by mating them with WT female mice. Conditional deletion of G3PP in the embryonic germ cells had no effect on the growth of the mice (data not shown) but led to a complete loss of fertility in the males. Although copulatory plugs were observed, no pups were produced, which indicated that the male cG3PP-KO mice were able to mate but were infertile. Even though Vasa-Cre directed gene deletion occurs in both male and female germ cells [35], we have focussed on the effects of G3PP deletion on male fertility rather than female fertility as G3PP expression is highest in the testis, whereas it is very low in ovaries (Gene Expression Database (GXD), Mouse Genome Informatics Web Site. (URL: http://www.informatics.jax.org) accessed 14 May 2024).

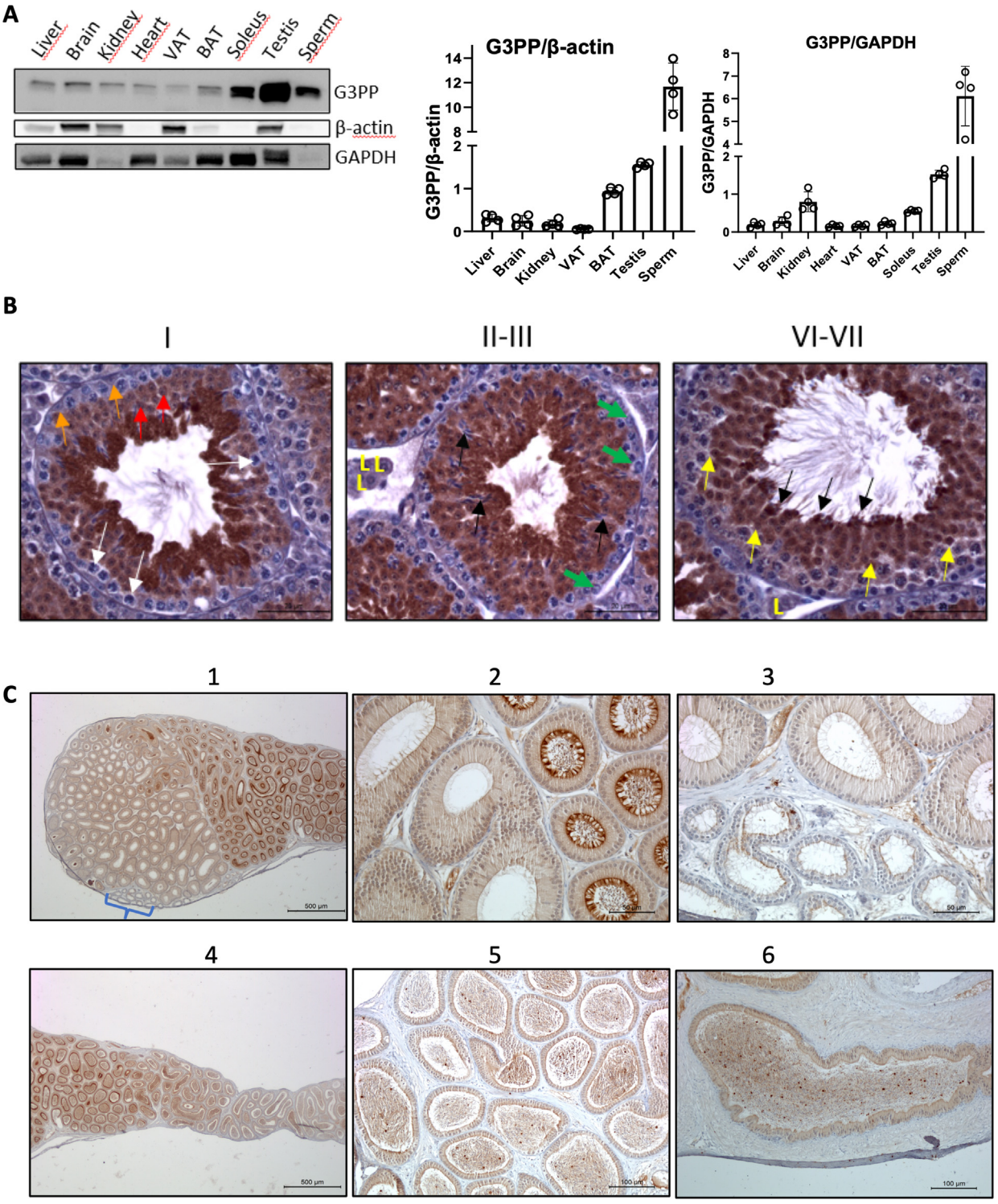

Figure 1: G3PP expression and histomorphological examination of the testis, epididymis, and sperm of WT mice. A. Western blot analysis of G3PP expression in various tissues of 3-month-old wild-type (WT) mice. G3PP expression was normalized to β-actin and GAPDH (n = 4); VAT, visceral adipose tissue; BAT, brown adipose tissue. **B.** Immunohistochemical staining of G3PP in the testis of WT mice across different stages of spermatogenesis. In the stage I, white arrows show G3PP-negative spermatocytes; red arrows indicate round spermatids; and orange arrows show Sertoli cells. In stages II-III green arrows show spermatogonia; black arrows point elongating spermatids; and Leydig cells indicated with "L". In stages VI-VII yellow arrows indicate spermatids that are G3PP-positive; and black arrows indicate elongating spermatids nearing the point of spermiation (which occurs at stage VIII), where the G3PP expression appears maximal. Scale bar = 20 μm for all panels. **C.** IHC staining of G3PP in the epididymis of WT mice. (1,2), Proximal caput (head) (left) and corpus (body) (right) regions viewed at both low (1) and high (2) magnification. G3PP expression specifically in the corpus is higher and mostly located in the luminal portion of the columnar cells and stereocilia. A small cluster of efferent ductules is also visible and indicated by the bracket in panel (1). (3), View of the interface between the efferent ductules (lower part of the panel) and the caput of the epididymis (upper part) taken at a higher magnification. The G3PP signal is relatively weak in the cilia of the efferent ductules, cytoplasm, and the stereocilia of principal cells of the epididymis. (4), View of the corpus and proximal cauda (tail) regions taken at low magnification, showing

3.4. Altered fertilization capacity and sperm parameters of cG3PP-KO mice

To further assess the fertilization capacity of the cG3PP-KO males, these mice were bred with superovulated WT females, and the resulting oocytes recovered and examined for the presence of cleavage to two-cell stage. The percentage of two-cell embryos scored 24h after mating was considered as the fertilization rate. Results showed that while the wild-type male mice had a 78% fertilization rate, the cG3PP-KO male mice were totally incapable of fertilizing oocytes even though these mice mated normally (Figure 3A). Furthermore, it was observed that the sperm from cG3PP-KO mice had diminished functionality and were abnormal. Thus, the total sperm motility of the cG3PP-KO mice was about 17-fold lower than that of the WT mice (Figure 3B), whereas the sperm capacitation was totally impaired (0%) in the cG3PP-KO mice compared to ∼50% capacitation in the WT mice (Figure 3C). The spontaneous acrosome reaction was 4-fold higher in the cG3PP-KO mouse sperm compared to WT (Figure 3D), indicating the instability of the acrosome. The impaired sperm motility and capacitation, and the high levels of spontaneous acrosome reaction suggest the inability of the cG3PP-KO spermatozoa to fertilize. Moreover, nearly 60% of the spermatozoa from the cauda epididymis of cG3PP-KO mice showed morphological abnormalities as compared to only ∼10% in the caudal spermatozoa from WT mice (Figure 3E). In addition, the caudal spermatozoa from cG3PP-KO mice showed elevated oxidative stress, as revealed by the significantly increased levels of 4-HNE, a lipid peroxidation product (Figure 3F). We then examined the testes from cG3PP-KO and floxed control mice to determine if there are any developmental defects in acrosome formation during spermatogenesis. Histological examination of the testes using PAS staining revealed no apparent morphological differences in the acrosome at all stages between control and cG3PP-KO mice (Figure 3G). Histological examination of the testes of the mutant mice showed no apparent morphologic defects of the germ cells despite the loss of G3PP (Figure 3G), indicating that the major degenerative processes that cause the abnormalities in the spermatozoa from the cG3PP-KO mice likely do not occur during spermatogenesis *per se,* but probably at other stages of spermatozoa maturation. Thus, the caudal spermatozoa from male mice with a loss of G3PP in the germinal cells right from the embryonic stage, are abnormal and show oxidative stress, and are incapable of fertilization.

3.5. Fertility in the icG3PP-KO male mice

As *Vasa* expression begins when the primordial germ cells colonize the gonad in mice and is detectable by e12.5 in both sexes and continues through the rest of the life, we chose transgenic Cre mice in which Cre expression is *Vasa* promoter (Ddx4) driven. However, cG3PP-KO mice were born in numbers about 20-fold lower than the expected Mendelian ratio, suggesting that high level of Cre expression in the germ cells of the male parent leads to the production of knockout embryos, which are not viable. In fact, constitutive whole-body G3PP deletion was earlier shown to cause embryonic lethality [47]. Because of this, we generated inducible conditional G3PP-KO mice (icG3PP-KO), in which G3PP deletion in germ cells occurs only upon the induction of Cre gene by tamoxifen. Unlike the cG3PP-KO male mice, the icG3PP-KO mice were able to breed normally and there was no effect on male fertility in terms of the number of litters and pups per litter (Supplementary Table 1). This was initially surprising as loss of G3PP protein in the sperm from icG3PP-KO mice was ∼90% (Figure 2C) as in the cG3PP-KO mouse testis. The unaltered fertility of the icG3PP-KO male mice is likely due to the significant level of residual normal sperm in the testis of these mice compared to the cG3PP-KO mice.

3.6. Altered sperm function parameters and oxidative stress of icG3PP-KO mice

Computer-assisted sperm analysis (CASA) of sperm collected from vehicle (corn oil) administered control mice ($G3PP^{flox/flox}$ mice and $G3PP^{flox/flox}$-Vasa-Cre mice, separately) and TMX-administered control ($G3PP^{flox/flox}$ mice) and $G3PP^{flox/flox}$-Vasa-Cre (icG3PP-KO) mice showed a significant reduction in total and progressive sperm motility in icG3PP-KO mice (Figure 4A,B). There was also a significant decline in the curvilinear velocity (VCL) (Figure 4C), which represents the rate of travel of the centroid of the sperm head during a certain time period, and in the straight-line (linear) velocity (VSL) (Figure 4E) of the icG3PP-KO sperm. In addition, a significant decrease was also noted in the straightness (STR) (Figure 4F), linearity of forward progression (LIN) (Figure 4G), and amplitude of lateral sperm head displacement (ALH) (Figure 4H) of the sperm, which is calculated from the amplitude of its lateral deviation from the cell's axis of progression. There was only a trend (not significant) for a reduced average path velocity (VAP) of the spermatozoa from icG3PP-KO mice compared to control mice (Figure 4D). There was a significantly greater number of abnormal spermatozoa in the icG3PP-KO mice compared to all controls (Figure 4I).

Sperm capacitation was markedly impaired for the icG3PP-KO spermatozoa compared to the other groups (Figure 4J). As seen in the case of cG3PP-KO mouse sperm, icG3PP-KO spermatozoa also displayed elevated spontaneous acrosomal reaction (Figure 4K) and oxidative stress as noted by increased (2—3 fold) production of 4-HNE (Figure 4L) and 8OHdG (Figure 4M). Even though, these results are similar to those with the spermatozoa from cG3PP-KO mice, there are some differences with regard to the motility and capacitation. These two parameters were almost completely suppressed in cG3PP-KO sperm, whereas in the icG3PP-KO sperm, there are few spermatozoa showing normal motility and capacitation compared to their corresponding controls.

3.7. Increased mitochondrial membrane potential and ROS levels in the icG3PP-KO mouse spermatozoa

Mitochondrial transmembrane potential ($\Delta\Psi_M$), which increases during respiration coupled electron transport in the mitochondrial inner membrane, is the main determining factor for ATP synthesis during oxidative phosphorylation. Mitochondria are considered to be the major source of ROS in most cells and the production of ROS is related to the $\Delta\Psi_M$ [48]. As we observed elevated oxidative stress in the icG3PP-KO spermatozoa, we explored the possibility of a disturbed mitochondrial $\Delta\Psi_M$ as the potential cause. We measured mitochondrial $\Delta\Psi_M$ in the sperm cells from control (TMX-administered $G3PP^{flox/flox}$ mice) and icG3PP-KO mice using a green monomeric fluorescent JC-1 dye, which accumulates in the

head-to-tail orientation from left-to-right. A progressive decrease in G3PP expression occurs from the corpus to the cauda, which is attributed to both the shortening and lower levels of G3PP expression in the stereocilia. (5), Higher magnification of interface between the corpus (left part) and cauda (right part) of the epididymis. (6), Vas deferens. Scale bars vary as follows: 500 μm for panels 1 and 4; 50 μm for 2 and 3; and 100 μm for 5 and 6. (For interpretation of the references to color/colour in this figure legend, the reader is referred to the Web version of this article.)

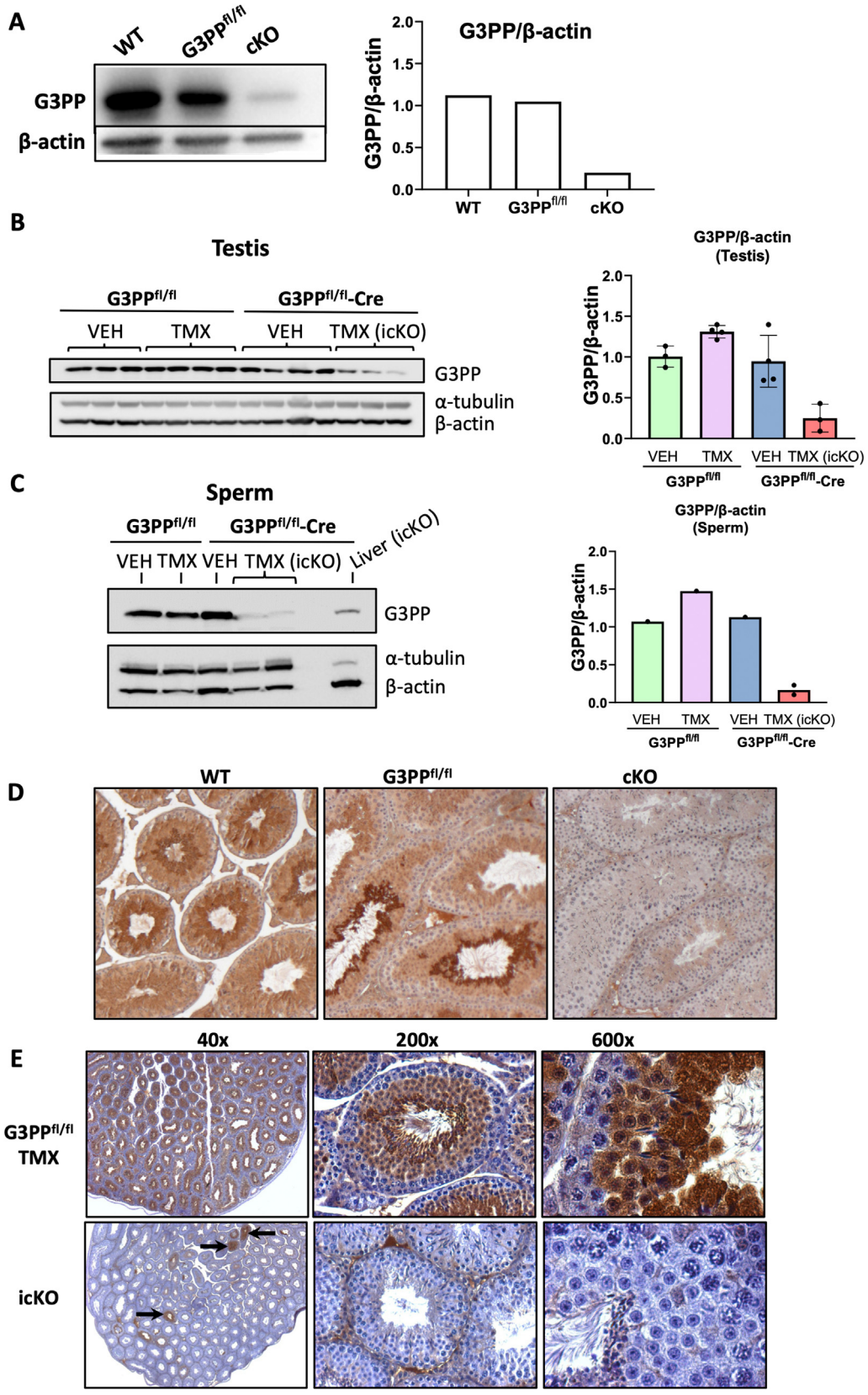

Figure 2: Validation of G3PP deletion in both the conditional and tamoxifen (TMX)-inducible G3PP-KO mice. A. Western blot for G3PP expression in whole testis lysates from WT, G3PP$^{flox/flox}$, and cG3PP-KO (G3PP$^{flox/flox}$-Vasa-Cre) mice. Densitometric analysis for G3PP expression normalized to β-actin is shown in the right panel. **B**–**C.** Western blot for G3PP expression in the TMX-inducible G3PP-KO mice. Whole testis protein lysates were prepared from TMX or corn oil (VEH) treated G3PP$^{flox/flox}$ (Flox-VEH and Flox-TMX) and G3PP$^{flox/flox}$-Vasa-CreERT2 (Flox-CreERT2-VEH and Flox-CreERT2-TMX) mice (**B**); and sperm isolated from the caudal epididymis (**C**). G3PP expression was normalized to both

mitochondrial matrix in proportion to the membrane potential and forms red fluorescent aggregates [49]. The results (Figure 4N) show that icG3PP-KO sperm mitochondria have significantly higher $\Delta\Psi_M$ compared to the TMX-administered G3PP$^{flox/flox}$ control mice. Elevated $\Delta\Psi_M$ permits high ATP synthesis and leads to elevated ROS production [49,50]. In the present study, ATP, ADP and AMP levels were unchanged in the icG3PP-KO sperm cells (Figure 5H—J). Therefore, we measured ROS production using DCFDA in the icG3PP-KO and control spermatozoa under the same conditions as for the mitochondrial $\Delta\Psi_M$ determination. The results showed much higher (4-fold) ROS levels in the icG3PP-KO spermatozoa (Figure 4O), suggesting that the increased mitochondrial $\Delta\Psi_M$ is directed towards elevated ROS production, which is the possible cause for the functional abnormality of the icG3PP-KO sperm.

3.8. Metabolic correlates of spermatozoa from icG3PP-KO mice

As mentioned above, the conditional deletion of G3PP in the germ cells had no apparent effect on spermatogenesis and the morphology of spermatozoa in testis, but impacted the spermatozoa collected from the KO mice. In order to understand the impact of G3PP deletion on spermatozoon metabolism, we conducted metabolic studies in the caudal spermatozoa from icG3PP-KO mice. The release of glycerol in the presence of 5.6 mM glucose into the medium following the incubation of the spermatozoa from icG3PP-KO mice was much lower compared to the control spermatozoa from tamoxifen-administered G3PP$^{flox/flox}$ mice (Figure 5A). These differences in glycerol release remained with the addition of fructose or increased level of glucose (Figure 5A). The results indicate that a significant portion of glycerol formed by spermatozoa arises from glucose via the hydrolysis of Gro3P formed during glycolysis and that this glycerol shunt is reduced in the sperm of icG3PP-KO mice.

We further conducted a targeted metabolomics analysis of the spermatozoa incubated in the presence of 5.6 mM glucose and 21.6 mM lactate, the same condition that is regularly used for capacitation and fertilization experiments (see methods). Deletion of G3PP led to an increase in Gro3P level in icG3PP-KO spermatozoa compared to control (Figure 5B), which is in agreement with the reduced glycerol production in these spermatozoa. However, there was no change in DHAP levels (Figure 5C). There were no differences between the groups in the levels of cellular redox determinants, including NAD/NADH, NADP/NADPH and GSSG/GSH (Figure 5 D-G; P,Q). Even though there was no change in the adenine nucleotide levels (Figure 5H—J), there was a significant decrease in the adenosine levels (Figure 5K) while cyclic AMP levels increased (Figure 5L) in icG3PP-KO compared to the control spermatozoa. Among the guanine nucletotides, only GMP showed an increase in the icG3PP-KO sperm (Figure 5O) and no changes in GDP and GTP (Figure 5M,N). Interestingly, all the analyzed amino acids, leucine, glutamate, glutamine, arginine and aspartate, increased the icG3PP-KO sperm compared to the control (Figure 5R—V), suggesting altered amino acid metabolism. The short-chain acyl-CoA, acetyl-CoA did not change (Figure 5W). Among the measured Krebs cycle intermediates, no changes were seen in succinate (Figure 5X), isocitrate (Figure 5Y) and malate showed a modest increase (Figure 5Z).

3.9. Abnormal sperm morphology of icG3PP-KO mice

Performing light microscopic examination, we observed that icG3PP-KO mice had high percentage of abnormal spermatozoa (Figure 4I) with folded flagella. However, there were still few normal appearing sperm cells (Figure 6A). It is known that in mice even a very small fraction of normal sperm is enough for normal fertility [51,52]. We further examined the icG3PP-KO spermatozoa by electron microscopy, which showed several major structural abnormalities. Unlike the vehicle-treated G3PP$^{flox/flox}$-Vasa Cre and TMX-treated G3PP$^{flox/flox}$ control mouse spermatozoa, the icG3PP-KO spermatozoa show a nucleus that is often distorted and also malformed acrosome, that is detached from the nuclear membrane (Figure 6B). In some icG3PP-KO mouse sperm cells, the nucleus is curved at the junction with the mid-piece and abnormally embedded in the cytoplasm (Figure 6C). In few icG3PP-KO spermatozoa, there is a misalignment of the mitochondria in the mid-piece with an excess of cytoplasm, misplacement of the principal piece, and a lack of the fibrous sheath and outer dense fiber (Figure 6 D, E). However, there are no gross structural abnormalities in mitochondrial structure in the icG3PP-KO spermatozoa (Figure 6C, D). As shown in Supplementary Tables 2, in the icG3PP-KO mouse spermatozoa, nearly 17% display normal morphology, compared to $\geq$ 80% normal sperm in the control mice.

4. DISCUSSION

Disturbed glycerol, glucose and lipid metabolism in sperm cells is known to perturb sperm functionality, leading to male infertility [8,9]. Several enzymes of glycerol metabolism, including GPD2 [53], GK [54,55], GPAT2 [56], and also the plasma membrane glycerol transporter AQP3 [10,12] have been found to have cardinal role in the maintenance of male fertility and normal sperm functions. It has been recently demonstrated that AQP7 is the major transporter of glycerol in human sperm [57], whereas AQP3 primarily conducts water efflux in the mouse sperm [58]. Indeed, conditions that lead to increased cellular levels of Gro3P, which is mostly generated via glycolysis, was suggested to negatively affect sperm capacitation [53]. Inasmuch as glycolysis is considered to be an essential source of ATP production in the principal piece of the spermatozoon [59], that is needed for sperm motility, altered metabolism of Gro3P is likely to impact sperm energetics and function. We recently discovered an important cytosolic enzyme, G3PP, that controls cellular levels of Gro3P, and thus participates in the overall regulation of intermediary and energy metabolism in several cell types [18—20,60]. Interestingly, G3PP was previously reported to be essential for embryo development in mice [47]. We now find that G3PP expression is highest in testis compared to all body tissues in the mice, with isolated sperm showing ~40-fold higher expression as compared to many tissues, which suggests an important role for this enzyme in sperm metabolism and function. The expression pattern of G3PP protein during spermatogenesis indicates that this enzyme likely plays an essential role in the late stages of sperm cell development and in mature spermatozoa.

To address the role of G3PP in sperm function and male fertility, we developed conditional G3PP-KO mice with specific deletion in the germ cells under the control of Ddx4 promoter from the embryonic stage (cG3PP-KO), as the whole-body G3PP-KO results in embryonic lethality

α-tubulin and β-actin for both testis and sperm Western blots. **D.** Validation of G3PP deletion in germ cells of cG3PP-KO mice by IHC of testes. G3PP staining was done on testis sections from 9-week-old WT, G3PP$^{flox/flox}$ control) and KO (G3PP$^{flox/flox}$-Vasa-Cre) mice. **E.** Validation of G3PP deletion in germ cells of icG3PP KO mice by IHC on testis sections. G3PP staining is shown at different levels of magnification. G3PP$^{flox/flox}$ mice treated with TMX (Flox-TMX) served as the control shown in the upper three panels, and the lower three panels show the KO group (G3PP$^{flox/flox}$-Vasa-CreERT2 mice treated with TMX).

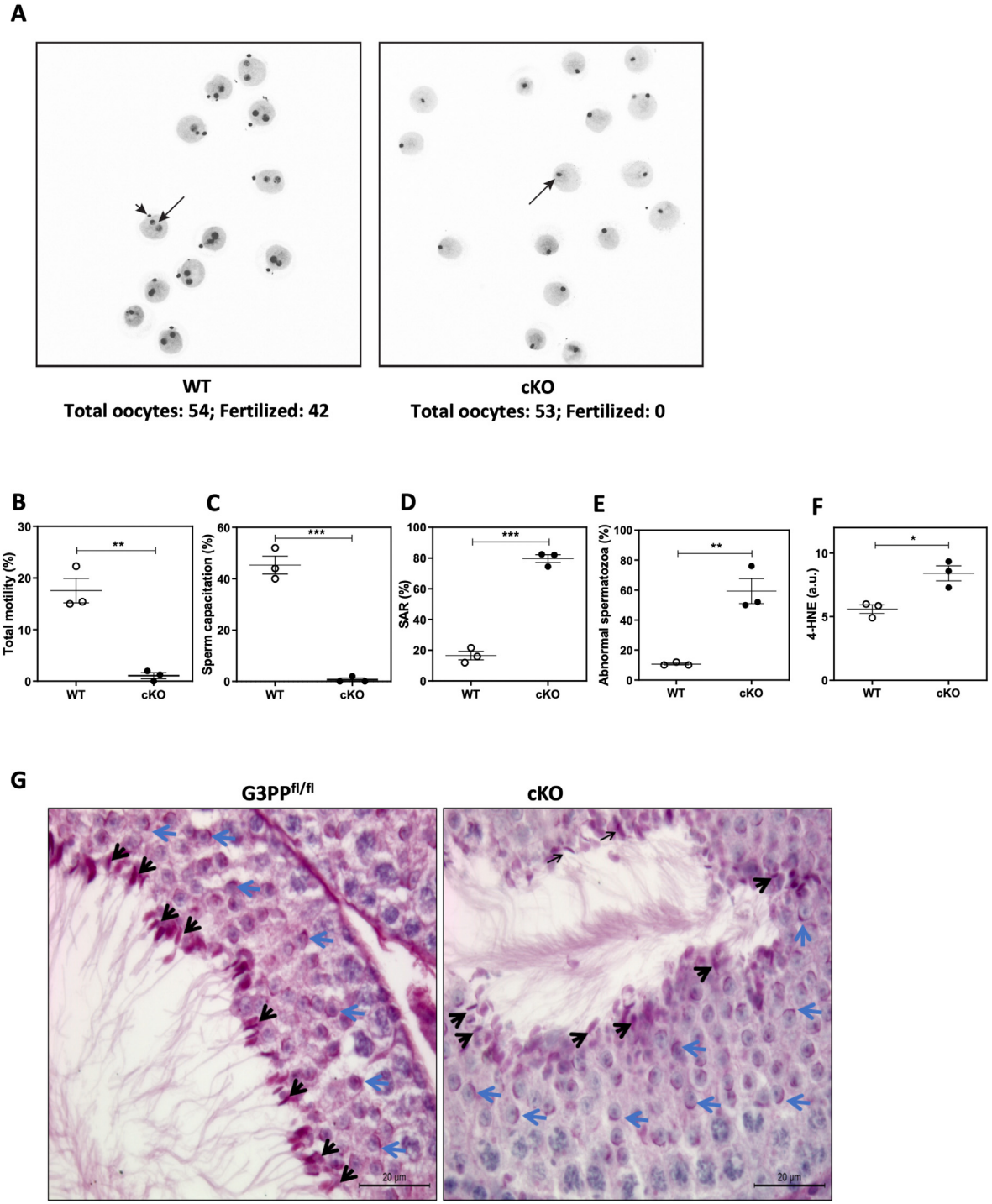

Figure 3: Deletion of G3PP in embryonic germ cells results in impaired sperm fertility and function. A. *In vivo* fertilization was used to assess the fertility of the cG3PP-KO mice. Superovulated WT females were mated to either WT or KO male mice and oocytes were recovered. Fertilization rate was considered as the percentage of two cell embryos scored 24 h after mating. Results show that the male KO mice have no capacity to fertilize oocytes. **B**–**F.** Measurement of various sperm function parameters in cG3PP-KO mice. **B**, Total sperm motility. **C**, % capacitation and **D**, % spontaneous–acrosome reaction (SAR). **E**, Abnormal spermatozoa (head, midpiece, and tail defects) as assessed by light microscopy. **F**, Levels of 4-HNE, a lipid peroxidation product. **G.** Acrosome morphology of control ($G3PP^{flox/flox}$) and cG3PP-KO mice, using PAS stain. Blue arrows show the acrosome as a thin purple crescent-shaped structure on the surface of round spermatids and black arrows indicate the elongating spermatids. Scale bar = 20 µm. Data shown in panels B to F represent mean ± SEM and were analyzed by unpaired two-tailed t-test (*$p < 0.05$, **$p < 0.01$, ***$p < 0.001$). (For interpretation of the references to color/colour in this figure legend, the reader is referred to the Web version of this article.)

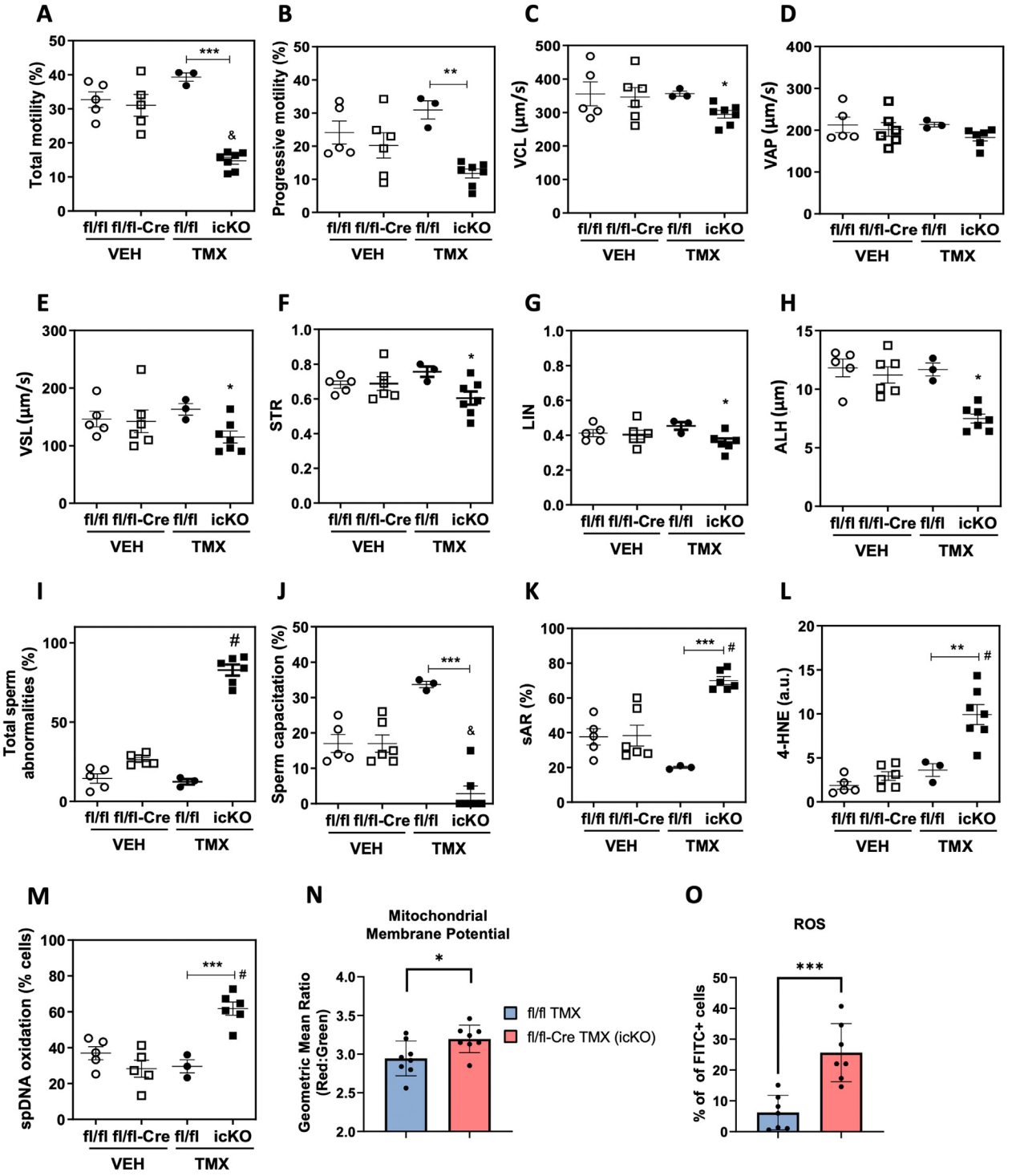

Figure 4: Abnormal sperm function parameters observed in the tamoxifen-inducible G3PP KO mice. A-L. Various sperm function parameters in icG3PP-KO mice were measured using a computer-assisted sperm analysis (CASA). **A**. Total motility, **B.** progressive motility, **C.** Curvilinear velocity (VCL), D. Average path velocity (VAP), **E.** Straight-line velocity (VSL), **F.** Straightness (STR), **G.** Linearity of forward progression (LIN) and **H.** Amplitude of lateral head displacement (ALH). **I.** Total sperm abnormalities, **J.** Sperm capacitation (%) and **K.** Spontaneous acrosome reaction (%SAR) were evaluated by determining the percentage of spermatozoa without acrosome by the Giemsa stain as described in Methods. **L.** Lipid peroxidation product 4-HNE and **M.** sperm DNA oxidation (8-dOHG) were measured using immunocytochemistry and relative intensity was assessed using ImageJ software. Data shown in panels **A-M** represent mean ± SEM and were analyzed by one-way ANOVA with Tukey's test. $^{**}p < 0.01$ and $^{***}p < 0.001$. "&" means lower compared to all other genotypes, whereas "#" means higher compared to all other genotypes. **N.** Membrane potential measured in sperm using JC-1 dye and flow cytometry. **O.** Reactive Oxygen Species (ROS) in the sperm were measured with DCFDA dye and flow cytometry. Data shown in panels **N** and **O** represent mean ± SEM and were analyzed by unpaired two-tailed t-test ($^{*}p < 0.05$ and $^{***}p < 0.001$).

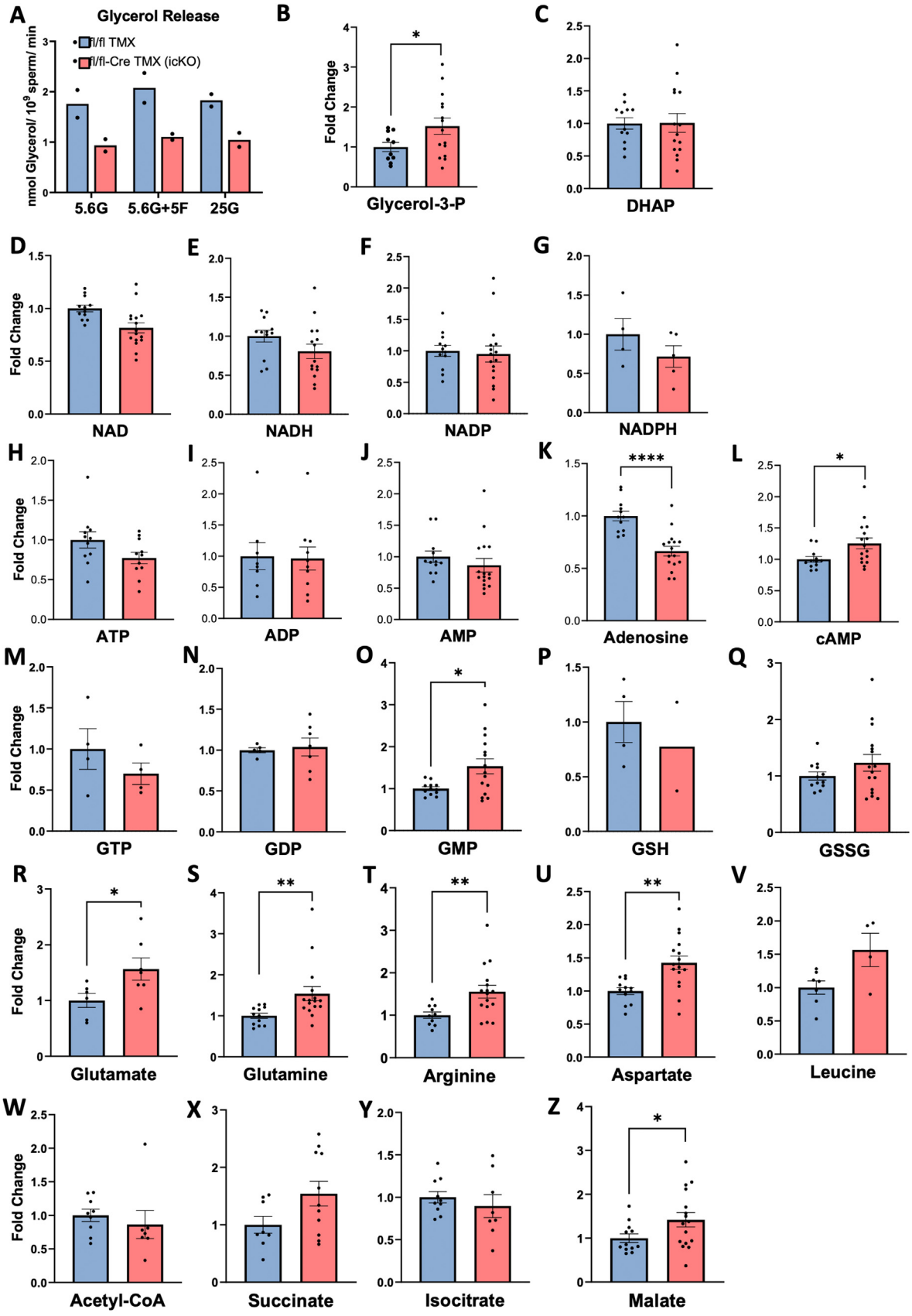

Figure 5: Metabolic alterations in the spermatozoa of inducible G3PP KO mice. A. Reduced glycerol release in the supernatant of sperm isolated from the caudal epididymis of icG3PP-KO mice. Results are from 2 independent experiments, measured in duplicate from two different pools of TMX-treated G3PP$^{flox/flox}$ (Flox-TMX) (total n = 6) and KO (Flox-

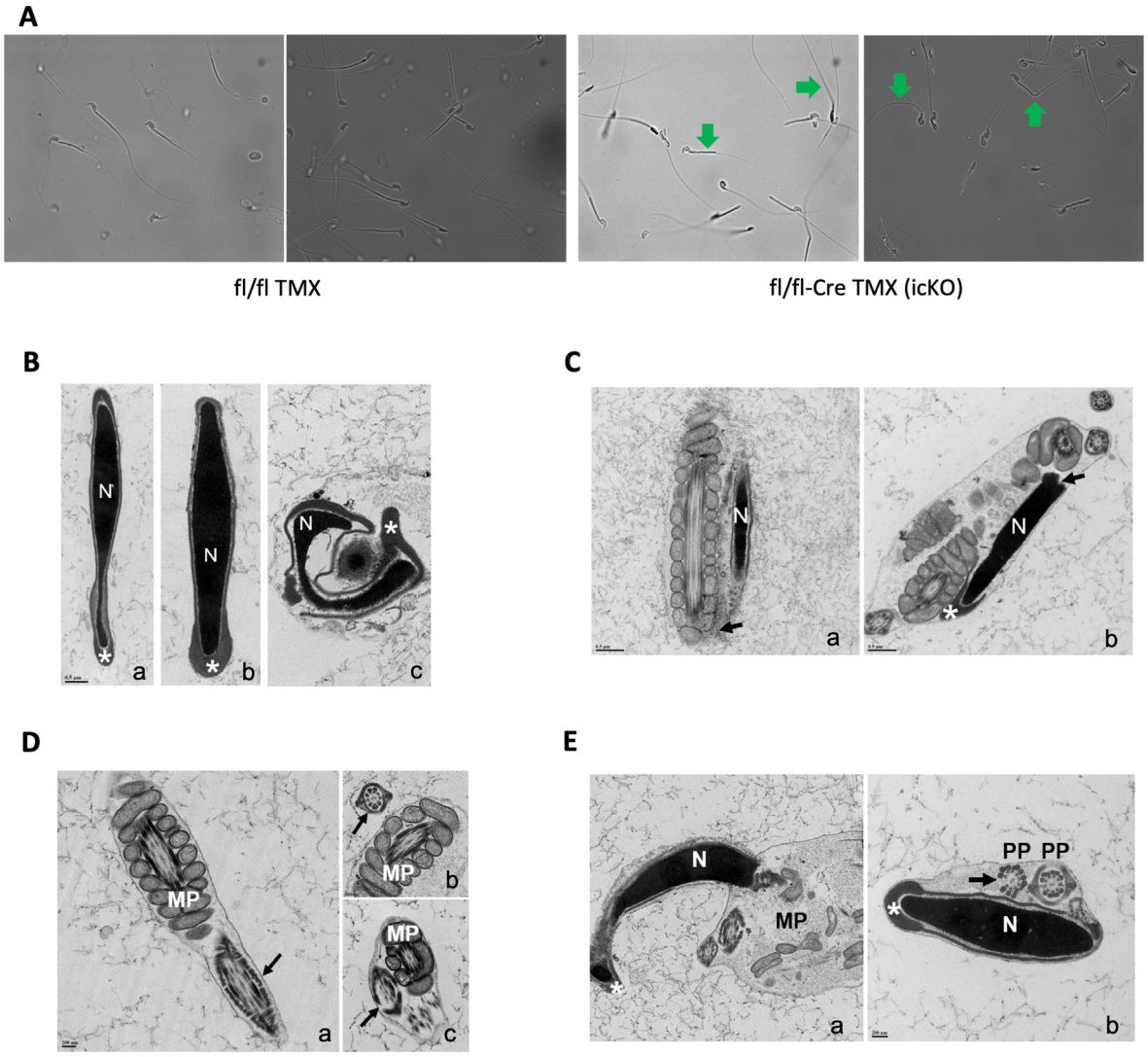

Figure 6: Microscopic examination of sperm from inducible G3PP KO mice. A. Abnormal folding of sperm observed in icG3PP KO mice. Representative light microscopic images of sperm from control (Flox-TMX) and KO (Flox-CreERT2-TMX) mice visualized at 40X magnification (n = 2). Arrows in the KO images point to sperm that appear normal and differ from abnormal sperm with folded/bent tails. **B.** Transmission electron microscopy (TEM) of mice sperm heads. *a*, Flox-CreERT2-VEH; *b*, Flox-TMX; *c*, KO. In *a* and *b*, the nuclei (N) and acrosomes (asterisks) do not present abnormalities. In *c*, the nucleus (N) is distorted, and the malformed acrosome (asterisk) is detached from the nuclear membrane. Scale bar = 0.5 μm applies to the 3 micrographs. **C.** TEM of spermatozoa from KO mice. In *a*, the sperm nucleus (N) is curved at the junction with the mid piece (arrow). In *b*, the sperm nucleus (N) is also bended at the neck (arrow) and abnormally embedded in cytoplasm. Scale bars = 0.5 μm. **D.** TEM of spermatozoa tails. *a*, Flox Cre VEH; *b*, Flox TMX; *c*, KO. In *a* and *b*, the mid (MP) and principal pieces (arrows) have normal appearance. In *c*, the principal piece is misplaced and mitochondria are misaligned in the mid piece with an excess of cytoplasm. Mitochondria in the midpiece appear normal in the control and KO sperm. Missing structural components of the fibrous sheath and axoneme (arrow) are noted. Scale bar = 200 nm applies to the 3 micrographs. **E.** TEM of sperm from KO mice. In *a*, the nucleus (N) and acrosome (asterisk) present normal appearances, but the mitochondria are not aligned in the mid-piece (MP). Note the excess of cytoplasm and the misplacement of the principal piece (PP). In *b*, the nucleus (N) and the acrosome (asterisk) also present a normal appearance. Note the misplacement of the principal piece and the absence of the fibrous sheath and one outer dense fiber (arrow). Scale bar = 200 nm applies to both micrographs.

[47]. The essential function of G3PP in male germ cells became evident as the male cG3PP-KO mice are completely sterile, whereas the fertility of female cG3PP-KO mice is unaffected. The sterility of the cG3PP-KO male mice appears to be due to an overall impaired sperm functionality as reflected by totally reduced motility and ability to undergo capacitation in spermatozoa, which also suffered from a much higher level of spontaneous acrosome reaction, the number of abnormal sperm cells and oxidative stress. Interestingly, a very similar phenotype was

ERT2Cre-TMX) (total n = 8) mice. Sperm were incubated in modified non-capacitated BWW medium with 5.6 mM glucose alone (5.6G), 5.6 mM glucose supplemented with 5 mM fructose (5.6G+5F), or 25 mM glucose (25G) for 1 h. **B-Z.** Levels of various metabolites including glycerol-3-phosphate (Glycerol-3-P; **B**), DHAP (**C**), NAD (**D**), NADH (**E**), NADP (**F**), NADPH (**G**), ATP (**H**), ADP (**I**), AMP (**J**), Adenosine (**K**), cAMP (**L**), GTP (**M**), GDP (**N**), GMP (**O**), Reduced glutathione (GSH; **P**), Oxidized glutathione (GSSG; **Q**), Glutamate (**R**), Glutamine (**S**), Arginine (**T**), Aspartate (**U**), Leucine (**V**), Acetyl-CoA (**W**), Succinate (×), Isocitrate (**Y**), and Malate (**Z**). Data are shown as mean ± SEM. Metabolite levels were analyzed by unpaired two-tailed t-test with Welch's correction (*$p < 0.05$, **$p < 0.01$, ****$p < 0.001$).

noticed in male mice with GPD2-KO, that have defective Gro3P and energy metabolism [53].

Further studies on the underlying molecular mechanism for the loss of male fertility were done using mice with tamoxifen-inducible deletion of G3PP in germ cells in male mice (icG3PP-KO), as the birth rate of cG3PP-KO mice was much lower than the expected Mendelian ratio, probably due to embryonic lethality, as noticed before [47]. Fertility of the icG3PP-KO male mice is not affected, unlike the cG3PP-KO male mice, and this is likely due to the observed presence of residual normal (wild-type) spermatozoa in the testis of these mice, as there is a noticeable level of G3PP protein in the testis and spermatzoa of the icG3PP-KO mice. In rodents, a reduction of more than 90% of sperm production is necessary to negatively affect fertility [61]. Nevertheless, the significantly reduced functional parameters of the sperm from icG3PP-KO mice indicated that the inducible deletion of G3PP leads to many abnormalities, as seen in the cG3PP-KO male mice and these defects are likely centered around disturbed metabolism and sperm morphology. Indeed, it has been shown that rapid progressive motility of the sperm with a forward progression by $\sim$25 μm/s in the cervical mucus is a determinant of the ability of the sperm to fertilize the egg efficiently [62] and these parameters are much reduced in the icG3PP-KO sperm. Thus, the motility, capacitation and acrosome reaction of the sperm are highly dependent on the energy metabolism and a balanced formation of ROS in the sperm [41,59,63] and the loss of G3PP likely compromised this equilibrium as evidenced by a rise in Gro3P level and mitochondrial membrane potential, as well as increased ROS levels, lipid (4-HNE level) and DNA (8OHdG level) peroxidation. Spermatozoa are rich in ω-6 polyunsaturated fatty acids, which are the prime source of 4-HNE during oxidative damage [64]. Capacitation is a metabolic energy-dependent series of biochemical and structural changes in the sperm and is a prerequisite for the acrosome reaction, which must be precisely timed for the sperm to be able to fertilize [65]. Capacitation is necessary to allow the spermatozoon to undergo acrosome reaction, the tightly-regulated exocytosis of the acrosome content to penetrate the zona pellucida and fertilize the egg. A premature release of acrosomal lytic enzymes due to acrosome membrane instability or impairment of capacitation results in spontaneous acrosome reaction, which leads to male sterility [66]. The defective acrosome reaction in the G3PP-KO spermatozoa is also likely due to the abnormalities in the morphology of the acrosome in the icG3PP-KO sperm, possibly caused by oxidative stress. Thus, while controlled and balanced production of ROS is necessary for optimal capacitation and properly timed acrosome reaction, increased ROS levels can have detrimental effects, leading to oxidative stress and premature spontaneous acrosome reaction [67]. Moreover, increased ROS production together with unaltered ATP levels can be a sign of the capacitation process, and we cannot exclude if the dysregulation of the sperm maturation process is the cause of premature capacitation. Oxidative stress promotes posttranslational protein modifications that impair sperm motility, capacitation, acrosome reaction and generates significant sperm DNA oxidation [41,43,68]. Moreover, male infertility is associated with high levels of ROS in the semen of infertile men [69], while ROS are undetectable in the semen of fertile men [70]. Interestingly, high-intensity radiation, which causes oxidative stress, was shown to elevate the expression of G3PP/PGP in the mouse testis [71], likely as a protective mechanism against stress, and we earlier showed that G3PP is a stress-inducible enzyme that plays a role in protection against diverse metabolic and environmental stresses [21–23]. In addition, elevated level of ROS, which causes DNA fragmentation as well as lipid peroxidation, is known to induce morphological and structural defects in the spermatozoa in patients with teratozoospermia and lead to male infertility [72,73] and to cause ferroptosis [5]. The structural abnormalities in the spermatozoa noticed by the light and electron microscopy in the cG3PP-KO and icG3PP-KO mice are most probably caused by the elevated production of ROS in these spermatozoa.

Mitochondria are the main source of ROS in most cells and the mitochondrial membrane potential ($\Delta\Psi_M$) is related to the production of ROS as well as ATP [48–50] in many cell types. In the present study the 4-fold increase in ROS levels in the icG3PP-KO spermatozoa without any change in the ATP levels, suggests that the increased mitochondrial $\Delta\Psi_M$ is directed primarily towards elevated ROS production, which possibly contributed to the functional abnormality of the icG3PP-KO spermatozoa. The significantly elevated $\Delta\Psi_M$ in the icG3PP-KO sperm mitochondria could have led to the increased ROS production and the resultant oxidative stress. The elevated Gro3P levels in the icG3PP-KO spermatozoa, likely drove the production of ROS via the mitochondrial GPD2 activity and the Gro3P redox shuttle. Mitochondrial GPD2 is known to be a major site of ROS production, as this enzyme transfers the electrons from cytosolic Gro3P to coenzyme Q of the mitochondrial electron transport chain, and coenzyme Q is the source of electron leakage and ROS production, and this step does not involve a global change in the redox status of the cell [74]. Indeed, isolated GPD2 is capable of generating ROS in the presence of coenzyme Q and in the absence of any other redox components [74]. It appears that G3PP participates in the sperm functions as a regulator of ROS production via Gro3P/GPD2, by hydrolyzing Gro3P to glycerol, which cannot be rephosphorylated to Gro3P by the spermatozoon as it does not have a catalytically active GK enzyme [75]. Even though, glycerol kinase-2 (GK2) and glycerol kinase-like 1 (Gykl1) proteins, which are similar to the classical glycerol kinase (GyK), have been shown to be present in the spermatozoa, unlike GyK, neither GK2 nor Gykl1 show any catalytic activity [76]. Nevertheless, these proteins were found to be important for spermatogenesis, probably playing some structural roles [54]. Exogenously added glycerol in boar spermatozoa was shown to be metabolized at low rates involving the formation of glyceraldehyde, then glyceraldehyde-3-phosphate, before entering glycolysis and further oxidation [31,33]. Thus, a lack of G3PP in the spermatozoa leads to elevated supply of Gro3P to mitochondrial GPD2, which in turn feeds these cytosolic electrons derived from Gro3P to coenzyme Q, which ultimately results in electron leakage and ROS production and associated cellular damage.

It was reported earlier [53,77] that GPD2 is localized mostly in the acrosomes and prinicipal piece, but not in the middle piece in mouse spermatozoa, and that its deletion results in reduced ROS and ATP production, negatively affecting the capacitation of the spermatozoa. In the present study, we did not investigate if GPD2 is localized in the mitochondria of spermatozoa. This raises the question on how GPD2 present in acrosomes or principal piece but not in mitochondria [53] contribute to ROS production? There is apparently a large amount ($\sim$63 mM) of glycerophosphocholine (GPC) in the epididymis lumen [78], which can be hydrolyzed by GPC phosphodiesterase (GDE), also present in epididymis [79], to give rise to Gro3P and choline. Thus, there can be a large supply of Gro3P to the spermatozoa during their maturation in the epididymis. Indeed spermatozoa can use externally added Gro3P efficiently via the action of GPD2 [32,33], possibly in the acrosomes and the principal piece [53]. This excess supply of Gro3P and its usage by the spermatozoa in epididymis needs to be controlled, by an enzyme like G3PP, which operates the glycerol shunt [19–21]. Absence of G3PP can lead to high levels of ROS production, in excess of what is normally needed for capacitation, via GPD2. This may be the reason for the apparent normal morphology of the G3PP-KO

spermatozoa when they are in testis, but abnormal morphology after they come through epididymis. However, this needs to be established in future studies. During the epididymal maturation of spermatozoa there are several metabolic changes that result in the production of ROS and their scavenging by the epididymal antioxidant enzymes [80]. Both the epididymal epithelial cells and spermatozoa generate their own ROS under normal physiological conditions [81], which at low and controlled levels act as second messengers in regulating signaling pathways in the epididymis [80]. As the spermatozoa have limited levels of the antioxidative enzymes needed to regulate ROS levels, the epididymal antioxidant machinery helps in maintaining ROS under control and in the protection of spermatozoa [82]. The elevated production of ROS due to the surplus supply of Gro3P in the epididymis, is likely also controlled by the epididymal G3PP, which is expressed at high levels in the corpus. However, in the spermatozoa, with limited levels of the antioxidative enzymes, G3PP is probably the major player to reduce the ROS production by hydrolyzing Gro3P.

Presently, it is difficult to pinpoint the precise stage(s) where the cellular damage occurs that is seen in the post epididymal spermatozoa, and further studies are needed to ascertain this. However, glycerol kinase protein is essential for forming the mitochondrial sheath in the spermatozoon during spermatogenesis [55]. Thus, the newly identified metabolic pathway in mammalian cells, the glycerol shunt operated by GPD1 and G3PP is essential in maintaining normal sperm function. Targeted metabolomics showing unchanged adenine and guanine nucleotides and Krebs cycle intermediates suggest that neither altered ATP production nor Krebs cycle appear to cause the defective sperm function in the icG3PP-KO mice. However, it is intriguing to note that the icG3PP-KO spermatozoa display a marked increase in several amino acids, suggesting an enhanced protein degradation in these sperm, likely caused by the noted oxidative stress. Important to note here is that 4-HNE, whose production is elevated in the icG3PP-KO spermatozoa, is known to bind with several proteins and flag them for proteasomal degradation and also apoptosis [64,83], which could have caused the elevated amino acids. In addition, ROS are known to activate proteolytic enzymes and to promote protein degradation which can alter various cellular functions [84].

Moreover, spermatozoa in the semen are also exposed to high fructose concentration, which reaches up to 15–20 mM [85], which is possibly the main source of energy, via glycolysis, for the spermatozoa. Fructose, via the formation of DHAP, is known to contribute to the production of glycating compounds such as methylglyoxal [86], which rapidly react with proteins and nucleic acids, causing their dysfunction. However, the presence of high levels of G3PP can be protective to spermatozoa, by diverting fructose as well as glucose carbons towards glycerol, away from DHAP/methylglyoxal formation. This potential role of G3PP in spermatozoon protection needs to be established. Why are G3PP expression levels so elevated in sperm? The glycerol shunt produces high amounts of glycerol, an osmolyte and cell-preserving agent [8,75]. We previously showed in *C.elegans* that the glycerol shunt protects the animal from many stresses (hyperosmotic, heat, oxidative and glucotoxic) [21,22]. G3PP is also essential for protecting fish and various insects from cold [87]. These stresses are relevant for sperm health and function in the male and female bodies. Indeed, during its journey to the egg, the spermatozoon is exposed to various stresses, including changes in osmolarity and pH, exposure to microorganisms, in entirely different milieux than in the testis or epididymis. Indeed, a recent study [10] suggested that the glycerol transporter AQP3 is essential for spermatozoa to cope with the progressive osmotic decrease through the female reproductive tract. AQP3-deficient mice show reduced sperm motility due to the inability of spermatozoa to regulate their volume, leading to tail deformations [58]. In addition, another aquaglyceroporin, AQP7, is expressed in human spermatozoa and is crucial for sperm motility [88]. Thus, the production and extracellular release of glycerol via AQPs by spermatozoa may be important for the maintenance of osmotic balance and functional integrity of the spermatozoa. Considering that spermatozoa have much lower triglyceride content [89], the major pathway for the production and release of glycerol is likely the G3PP/glycerol shunt, and a lack of G3PP may adversely affect the function of spermatozoa, as noticed in the present study. We propose that high G3PP and glycerol production favor sperm preservation via both intra- and extracellular actions. This merits further investigation as it has implications for fertility.

Overall, the present study demonstrates an important role for G3PP-operated glycerol shunt in regulating sperm Gro3P levels, which, if not controlled, can lead to excess ROS production, altered sperm morphology and function and eventual male infertility. A lack of G3PP in spermatozoa appears to disturb glucose, amino acid, lipid and energy metabolism, probably due to the dysregulation of Gro3P, which is at the center of all these metabolic pathways. Such a regulatory role of G3PP in controlling metabolism and ROS production may possibly explain the increased incidence of male infertility among diabetics and obese people with elevated circulating glucose [3], which is the main source of cellular Gro3P. The relevance of these results to human health is exemplified by the recent study showing that G3PP expression is reduced by ~50-fold in the sperm from testicular seminoma patients with reduced fertility compared to sperm from healthy men [27]. Thus, future studies are warranted to closely examine the importance of G3PP in male fertility in human subjects and if pharmacological augmentation of this enzyme is a therapeutic avenue to prevent any oxidative damage to the susceptible sperm, as in the case of patients with diabetes.

CRediT AUTHORSHIP CONTRIBUTION STATEMENT

Abel Oppong: Writing – original draft, Methodology, Formal analysis, Data curation. **Yat Hei Leung:** Methodology, Formal analysis. **Anindya Ghosh:** Methodology, Formal analysis, Data curation. **Marie-Line Peyot:** Investigation, Formal analysis, Data curation. **Marilène Paquet:** Methodology, Formal analysis. **Carlos Morales:** Methodology, Formal analysis, Data curation. **Hugh J. Clarke:** Methodology, Investigation, Formal analysis. **Fahd Al-Mulla:** Writing – review & editing, Funding acquisition. **Alexandre Boyer:** Resources, Methodology, Investigation, Formal analysis, Conceptualization. **S. R. Murthy Madiraju:** Writing – review & editing, Writing – original draft, Supervision, Resources, Project administration, Methodology, Investigation, Funding acquisition, Formal analysis, Data curation, Conceptualization. **Derek Boerboom:** Writing – review & editing, Resources, Methodology, Investigation, Formal analysis, Data curation, Conceptualization. **Cristian O'Flaherty:** Resources, Project administration, Methodology, Investigation, Funding acquisition, Formal analysis, Data curation, Conceptualization. **Marc Prentki:** Writing – review & editing, Writing – original draft, Supervision, Resources, Project administration, Methodology, Investigation, Funding acquisition, Formal analysis, Data curation, Conceptualization.

ACKNOWLEDGMENTS

This work was supported by funds from the Canadian Institutes of Health Research (to M.P., S.R.M.M.) and Dasman Diabetes Research Institute/Montreal Medical International (to M.P., S.R.M.M., F.A-M.). This study was partially funded by a CIHR grant to C. O'F. We thank

the core facilities and the animal house facility of CRCHUM. We are grateful to Ms. Jeannie Mui for her technical assistance and the EM work was partially supported by an NSERC grant to Carlos R. Morales. We thank Hao-Yu Liao and Francis Marien-Bourgeois for their technical assistance.

DECLARATION OF COMPETING INTEREST

The authors declare that they have no known competing financial interests or personal relationships that could have appeared to influence the work reported in this paper.

APPENDIX A. SUPPLEMENTARY DATA

Supplementary data to this article can be found online at https://doi.org/10.1016/j.molmet.2024.102063.

DATA AVAILABILITY

Data will be made available on request.

REFERENCES

[1] Barratt CLR, De Jonge CJ, Sharpe RM. 'Man Up': the importance and strategy for placing male reproductive health centre stage in the political and research agenda. Hum Reprod 2018;33(4):541–5.
[2] Skakkebaek NE, Rajpert-De Meyts E, Buck Louis GM, Toppari J, Andersson AM, Eisenberg ML, et al. Male reproductive disorders and fertility trends: influences of environment and genetic susceptibility. Physiol Rev 2016;96(1):55–97.
[3] Alves MG, Jesus TT, Sousa M, Goldberg E, Silva BM, Oliveira PF. Male fertility and obesity: are ghrelin, leptin and glucagon-like peptide-1 pharmacologically relevant? Curr Pharmaceut Des 2016;22(7):783–91.
[4] Carrageta DF, Pereira SC, Ferreira R, Monteiro MP, Oliveira PF, Alves MG. Signatures of metabolic diseases on spermatogenesis and testicular metabolism. Nat Rev Urol 2024;21(8):477–94.
[5] Martin-Cano FE, Gaitskell-Phillips G, da Silva-Alvarez E, Silva-Rodriguez A, Castillejo-Rufo A, Tapia JA, et al. The concentration of glucose in the media influences the susceptibility of stallion spermatozoa to ferroptosis. Reproduction 2024;167(1).
[6] Ortiz-Rodriguez JM, Martin-Cano FE, Gaitskell-Phillips GL, Silva A, Ortega-Ferrusola C, Gil MC, et al. Low glucose and high pyruvate reduce the production of 2-oxoaldehydes, improving mitochondrial efficiency, redox regulation, and stallion sperm functiondagger. Biol Reprod 2021;105(2):519–32.
[7] Park YJ, Pang MG. Mitochondrial functionality in male fertility: from spermatogenesis to fertilization. Antioxidants 2021;10(1).
[8] Crisostomo L, Alves MG, Calamita G, Sousa M, Oliveira PF. Glycerol and testicular activity: the good, the bad and the ugly. Mol Hum Reprod 2017;23(11):725–37.
[9] Wiebe JP, Kowalik A, Gallardi RL, Egeler O, Clubb BH. Glycerol disrupts tight junction-associated actin microfilaments, occludin, and microtubules in Sertoli cells. J Androl 2000;21(5):625–35.
[10] Mohammadi P, Mesbah-Namin SA, Movahedin M. Attenuation of aquaporin-3 may be contributing to low sperm motility and is associated with activated caspase-3 in asthenozoospermic individuals. Andrologia 2021;53(8):e14119.
[11] Yeung CH. Aquaporins in spermatozoa and testicular germ cells: identification and potential role. Asian J Androl 2010;12(4):490–9.
[12] Alyasin A, Momeni HR, Mahdieh M. Aquaporin3 expression and the potential role of aquaporins in motility and mitochondrial membrane potential in human spermatozoa. Andrologia 2020;52(6):e13588.
[13] Laforenza U, Pellavio G, Marchetti AL, Omes C, Todaro F, Gastaldi G. Aquaporin-mediated water and hydrogen peroxide transport is involved in normal human spermatozoa functioning. Int J Mol Sci 2016;18(1):66.
[14] Moretti E, Terzuoli G, Mazzi L, Iacoponi F, Collodel G. Immunolocalization of aquaporin 7 in human sperm and its relationship with semen parameters. Syst Biol Reprod Med 2012;58(3):129–35.
[15] Prentki M, Madiraju SR. Glycerolipid metabolism and signaling in health and disease. Endocr Rev 2008;29(6):647–76.
[16] Klein S, Weber JM, Coyle EF, Wolfe RR. Effect of endurance training on glycerol kinetics during strenuous exercise in humans. Metabolism 1996;45(3):357–61.
[17] Zhao S, Mugabo Y, Iglesias J, Xie L, Delghingaro-Augusto V, Lussier R, et al. alpha/beta-Hydrolase domain-6-accessible monoacylglycerol controls glucose-stimulated insulin secretion. Cell Metabol 2014;19(6):993–1007.
[18] Mugabo Y, Zhao S, Seifried A, Gezzar S, Al-Mass A, Zhang D, et al. Identification of a mammalian glycerol-3-phosphate phosphatase: role in metabolism and signaling in pancreatic beta-cells and hepatocytes. Proc Natl Acad Sci U S A 2016;113(4):E430–9.
[19] Al-Mass A, Poursharifi P, Peyot ML, Lussier R, Levens EJ, Guida J, et al. Glycerol-3-phosphate phosphatase operates a glycerol shunt in pancreatic β-cells that controls insulin secretion and metabolic stress. Mol Metabol 2022;60:101471.
[20] Al-Mass A, Poursharifi P, Peyot ML, Lussier R, Chenier I, Leung YH, et al. Hepatic glycerol shunt and glycerol-3-phosphate phosphatase control liver metabolism and glucodetoxification under hyperglycemia. Mol Metabol 2022;66:101609.
[21] Possik E, Klein LL, Sanjab P, Zhu R, Cote L, Bai Y, et al. Glycerol 3-phosphate phosphatase/PGPH-2 counters metabolic stress and promotes healthy aging via a glycogen sensing-AMPK-HLH-30-autophagy axis in C. elegans. Nat Commun 2023;14(1):5214.
[22] Possik E, Schmitt C, Al-Mass A, Bai Y, Cote L, Morin J, et al. Phosphoglycolate phosphatase homologs act as glycerol-3-phosphate phosphatase to control stress and healthspan in C. elegans. Nat Commun 2022;13(1):177.
[23] Possik E, Al-Mass A, Peyot ML, Ahmad R, Al-Mulla F, Madiraju SRM, et al. New mammalian glycerol-3-phosphate phosphatase: role in beta-cell, liver and adipocyte metabolism. Front Endocrinol 2021;12:706607.
[24] Possik E, Madiraju SRM, Prentki M. Glycerol-3-phosphate phosphatase/PGP: role in intermediary metabolism and target for cardiometabolic diseases. Biochimie 2017;143:18–28.
[25] Platts AE, Dix DJ, Chemes HE, Thompson KE, Goodrich R, Rockett JC, et al. Success and failure in human spermatogenesis as revealed by teratozoospermic RNAs (Supplementary material on GeoProfiles). Hum Mol Genet 2007;16(7):763–73.
[26] Wang Z, Ding Z, Guan Y, Liu C, Wang L, Shan W, et al. Altered gene expression in the testis of infertile patients with nonobstructive azoospermia. Comput Math Methods Med 2021;2021:5533483.
[27] Dias TR, Agarwal A, Pushparaj PN, Ahmad G, Sharma R. Reduced semen quality in patients with testicular cancer seminoma is associated with alterations in the expression of sperm proteins. Asian J Androl 2020;22(1):88–93.
[28] Masaki H, Kim N, Nakamura H, Kumasawa K, Kamata E, Hirano KI, et al. Long-chain fatty acid triglyceride (TG) metabolism disorder impairs male fertility: a study using adipose triglyceride lipase deficient mice. Mol Hum Reprod 2017;23(7):452–60.
[29] Osuga J, Ishibashi S, Oka T, Yagyu H, Tozawa R, Fujimoto A, et al. Targeted disruption of hormone-sensitive lipase results in male sterility and adipocyte hypertrophy, but not in obesity. Proc Natl Acad Sci U S A 2000;97(2):787–92.

[30] Taschler U, Radner FP, Heier C, Schreiber R, Schweiger M, Schoiswohl G, et al. Monoglyceride lipase deficiency in mice impairs lipolysis and attenuates diet-induced insulin resistance. J Biol Chem 2011;286(20):17467–77.
[31] Jones AR, Chantrill LA, Cokinakis A. Metabolism of glycerol by mature boar spermatozoa. J Reprod Fertil 1992;94(1):129–34.
[32] Jones AR, Bubb WA. Substrates for endogenous metabolism by mature boar spermatozoa. J Reprod Fertil 2000;119(1):129–35.
[33] Jones AR, Gillan L. Metabolism of glycerol 3-phosphate by mature boar spermatozoa. J Reprod Fertil 1996;106(2):321–7.
[34] Takeshima T, Usui K, Mori K, Asai T, Yasuda K, Kuroda S, et al. Oxidative stress and male infertility. Reprod Med Biol 2021;20(1):41–52.
[35] Gallardo T, Shirley L, John GB, Castrillon DH. Generation of a germ cell-specific mouse transgenic Cre line, Vasa-Cre. Genesis 2007;45(6):413–7.
[36] John GB, Gallardo TD, Shirley LJ, Castrillon DH. Foxo3 is a PI3K-dependent molecular switch controlling the initiation of oocyte growth. Dev Biol 2008;321(1):197–204.
[37] Zudova D, Wyrobek AJ, Bishop J, Marchetti F. Impaired fertility in T-stock female mice after superovulation. Reproduction 2004;128(5):573–81.
[38] Bedard N, Yang Y, Gregory M, Cyr DG, Suzuki J, Yu X, et al. Mice lacking the USP2 deubiquitinating enzyme have severe male subfertility associated with defects in fertilization and sperm motility. Biol Reprod 2011;85(3):594–604.
[39] Wang Y. Epididymal sperm count. Curr Protoc Toxicol Chapter 2003;16.
[40] Ozkosem B, Feinstein SI, Fisher AB, O'Flaherty C. Advancing age increases sperm chromatin damage and impairs fertility in peroxiredoxin 6 null mice. Redox Biol 2015;5:15–23.
[41] Ozkosem B, Feinstein SI, Fisher AB, O'Flaherty C. Absence of peroxiredoxin 6 amplifies the effect of oxidant stress on mobility and SCSA/CMA3 defined chromatin quality and impairs fertilizing ability of mouse spermatozoa. Biol Reprod 2016;94(3):68.
[42] Moawad AR, Fernandez MC, Scarlata E, Dodia C, Feinstein SI, Fisher AB, et al. Deficiency of peroxiredoxin 6 or inhibition of its phospholipase A(2) activity impair the in vitro sperm fertilizing competence in mice. Sci Rep 2017;7(1):12994.
[43] Bumanlag E, Scarlata E, O'Flaherty C. Peroxiredoxin 6 peroxidase and Ca(2+)-independent phospholipase A(2) activities are essential to support male-mouse fertility. Antioxidants 2022;11(2).
[44] Scarlata E, Fernandez MC, O'Flaherty C. A novel combination of gamma-tocopherol-rich mixture of tocopherols and ascorbic acid restores fertility in cases of tyrosine nitration-associated male infertility in mice. Antioxidants 2020;9(7).
[45] Guo J, Grow EJ, Mlcochova H, Maher GJ, Lindskog C, Nie X, et al. The adult human testis transcriptional cell atlas. Cell Res 2018;28(12):1141–57.
[46] Guo J, Nie X, Giebler M, Mlcochova H, Wang Y, Grow EJ, et al. The dynamic transcriptional cell atlas of testis development during human puberty. Cell Stem Cell 2020;26(2):262–276 e264.
[47] Segerer G, Hadamek K, Zundler M, Fekete A, Seifried A, Mueller MJ, et al. An essential developmental function for murine phosphoglycolate phosphatase in safeguarding cell proliferation. Sci Rep 2016;6:35160.
[48] Korshunov SS, Skulachev VP, Starkov AA. High protonic potential actuates a mechanism of production of reactive oxygen species in mitochondria. FEBS Lett 1997;416(1):15–8.
[49] Suski J, Lebiedzinska M, Bonora M, Pinton P, Duszynski J, Wieckowski MR. Relation between mitochondrial membrane potential and ROS formation. Methods Mol Biol 2018;1782:357–81.
[50] Wojtczak L, Teplova VV, Bogucka K, Czyz A, Makowska A, Wieckowski MR, et al. Effect of glucose and deoxyglucose on the redistribution of calcium in ehrlich ascites tumour and Zajdela hepatoma cells and its consequences for mitochondrial energetics. Further arguments for the role of Ca(2+) in the mechanism of the crabtree effect. Eur J Biochem 1999;263(2):495–501.
[51] Santti H, Mikkonen L, Anand A, Hirvonen-Santti S, Toppari J, Panhuysen M, et al. Disruption of the murine PIASx gene results in reduced testis weight. J Mol Endocrinol 2005;34(3):645–54.
[52] Zhang C, Yeh S, Chen YT, Wu CC, Chuang KH, Lin HY, et al. Oligozoospermia with normal fertility in male mice lacking the androgen receptor in testis peritubular myoid cells. Proc Natl Acad Sci U S A 2006;103(47):17718–23.
[53] Kota V, Rai P, Weitzel JM, Middendorff R, Bhande SS, Shivaji S. Role of glycerol-3-phosphate dehydrogenase 2 in mouse sperm capacitation. Mol Reprod Dev 2010;77(9):773–83.
[54] Chen Y, Liang P, Huang Y, Li M, Zhang X, Ding C, et al. Glycerol kinase-like proteins cooperate with Pld6 in regulating sperm mitochondrial sheath formation and male fertility. Cell Discov 2017;3:17030.
[55] Shimada K, Kato H, Miyata H, Ikawa M. Glycerol kinase 2 is essential for proper arrangement of crescent-like mitochondria to form the mitochondrial sheath during mouse spermatogenesis. J Reprod Dev 2019;65(2):155–62.
[56] Garcia-Fabiani MB, Montanaro MA, Stringa P, Lacunza E, Cattaneo ER, Santana M, et al. Glycerol-3-phosphate acyltransferase 2 is essential for normal spermatogenesis. Biochem J 2017;474(18):3093–107.
[57] Ribeiro JC, Bernardino RL, Goncalves A, Barros A, Calamita G, Alves MG, et al. Aquaporin-7-Mediated glycerol permeability is linked to human sperm motility in asthenozoospermia and during sperm capacitation. Cells 2023;12(15).
[58] Chen Q, Peng H, Lei L, Zhang Y, Kuang H, Cao Y, et al. Aquaporin3 is a sperm water channel essential for postcopulatory sperm osmoadaptation and migration. Cell Res 2011;21(6):922–33.
[59] Amaral A. Energy metabolism in mammalian sperm motility. WIREs Mech Dis 2022;14(5):e1569.
[60] Lounis MA, Ouellet V, Peant B, Caron C, Li Z, Al-Mass A, et al. Elevated expression of glycerol-3-phosphate phosphatase as a biomarker of poor prognosis and aggressive prostate cancer. Cancers 2021;13(6).
[61] Robaire B, Smith S, Hales BF. Suppression of spermatogenesis by testosterone in adult male rats: effect on fertility, pregnancy outcome and progeny. Biol Reprod 1984;31(2):221–30.
[62] Bjorndahl L. The usefulness and significance of assessing rapidly progressive spermatozoa. Asian J Androl 2010;12(1):33–5.
[63] Rato L, Alves MG, Socorro S, Duarte AI, Cavaco JE, Oliveira PF. Metabolic regulation is important for spermatogenesis. Nat Rev Urol 2012;9(6):330–8.
[64] Bromfield EG, Aitken RJ, McLaughlin EA, Nixon B. Proteolytic degradation of heat shock protein A2 occurs in response to oxidative stress in male germ cells of the mouse. Mol Hum Reprod 2017;23(2):91–105.
[65] Menkveld R, Stander FS, Kotze TJ, Kruger TF, van Zyl JA. The evaluation of morphological characteristics of human spermatozoa according to stricter criteria. Hum Reprod 1990;5(5):586–92.
[66] Tesarik J. Appropriate timing of the acrosome reaction is a major requirement for the fertilizing spermatozoon. Hum Reprod 1989;4(8):957–61.
[67] Hsu PC, Hsu CC, Guo YL. Hydrogen peroxide induces premature acrosome reaction in rat sperm and reduces their penetration of the zona pellucida. Toxicology 1999;139(1–2):93–101.
[68] Morielli T, O'Flaherty C. Oxidative stress impairs function and increases redox protein modifications in human spermatozoa. Reproduction 2015;149(1):113–23.
[69] Yumura Y, Takeshima T, Kawahara T, Sanjo H, Kuroda SN, Asai T, et al. Reactive oxygen species measured in the unprocessed semen samples of 715 infertile patients. Reprod Med Biol 2017;16(4):354–63.
[70] Agarwal A, Sharma RK, Nallella KP, Thomas Jr AJ, Alvarez JG, Sikka SC. Reactive oxygen species as an independent marker of male factor infertility. Fertil Steril 2006;86(4):878–85.
[71] Li H, Zhang H, Xie Y, He Y, Miao G, Yang L, et al. Proteomic analysis for testis of mice exposed to carbon ion radiation. Mutat Res 2013;755(2):148–55.
[72] Oumaima A, Tesnim A, Zohra H, Amira S, Ines Z, Sana C, et al. Investigation on the origin of sperm morphological defects: oxidative attacks, chromatin immaturity, and DNA fragmentation. Environ Sci Pollut Res Int 2018;25(14):13775–86.

[73] O'Flaherty C, Scarlata E. Oxidative stress and reproductive function: the protection of mammalian spermatozoa against oxidative stress. Reproduction 2022;164(6):F67—78.
[74] Mracek T, Holzerova E, Drahota Z, Kovarova N, Vrbacky M, Jesina P, et al. ROS generation and multiple forms of mammalian mitochondrial glycerol-3-phosphate dehydrogenase. Biochim Biophys Acta 2014;1837(1):98—111.
[75] Lin EC. Glycerol utilization and its regulation in mammals. Annu Rev Biochem 1977;46:765—95.
[76] Pan Y, Decker WK, Huq AH, Craigen WJ. Retrotransposition of glycerol kinase-related genes from the X chromosome to autosomes: functional and evolutionary aspects. Genomics 1999;59(3):282—90.
[77] Kota V, Dhople VM, Shivaji S. Tyrosine phosphoproteome of hamster spermatozoa: role of glycerol-3-phosphate dehydrogenase 2 in sperm capacitation. Proteomics 2009;9(7):1809—26.
[78] Cooper TG, Brooks DE. Entry of glycerol into the rat epididymis and its utilization by epididymal spermatozoa. J Reprod Fertil 1981;61(1):163—9.
[79] Ohshima N, Kudo T, Yamashita Y, Mariggio S, Araki M, Honda A, et al. New members of the mammalian glycerophosphodiester phosphodiesterase family: GDE4 and GDE7 produce lysophosphatidic acid by lysophospholipase D activity. J Biol Chem 2015;290(7):4260—71.
[80] Weigel Munoz M, Cohen DJ, Da Ros VG, Gonzalez SN, Rebagliati Cid A, Sulzyk V, et al. Physiological and pathological aspects of epididymal sperm maturation. Mol Aspect Med 2024;100:101321.
[81] Vernet P, Fulton N, Wallace C, Aitken RJ. Analysis of reactive oxygen species generating systems in rat epididymal spermatozoa. Biol Reprod 2001;65(4):1102—13.
[82] O'Flaherty C. Orchestrating the antioxidant defenses in the epididymis. Andrology 2019;7(5):662—8.
[83] Aitken RJ, Whiting S, De Iuliis GN, McClymont S, Mitchell LA, Baker MA. Electrophilic aldehydes generated by sperm metabolism activate mitochondrial reactive oxygen species generation and apoptosis by targeting succinate dehydrogenase. J Biol Chem 2012;287(39):33048—60.
[84] Powers SK, Ozdemir M, Hyatt H. Redox control of proteolysis during inactivity-induced skeletal muscle atrophy. Antioxidants Redox Signal 2020;33(8):559—69.
[85] Owen DH, Katz DF. A review of the physical and chemical properties of human semen and the formulation of a semen simulant. J Androl 2005;26(4):459—69.
[86] Wei Y, Wang D, Moran G, Estrada A, Pagliassotti MJ. Fructose-induced stress signaling in the liver involves methylglyoxal. Nutr Metab 2013;10:32.
[87] Ditlecadet D, Driedzic WR. Glycerol-3-phosphatase and not lipid recycling is the primary pathway in the accumulation of high concentrations of glycerol in rainbow smelt (Osmerus mordax). Am J Physiol Regul Integr Comp Physiol 2013;304(4):R304—12.
[88] Saito K, Kageyama Y, Okada Y, Kawakami S, Kihara K, Ishibashi K, et al. Localization of aquaporin-7 in human testis and ejaculated sperm: possible involvement in maintenance of sperm quality. J Urol 2004;172(5 Pt 1):2073—6.
[89] Furse S, Kusinski LC, Ray A, Glenn-Sansum C, Williams HEL, Koulman A, et al. Relative abundance of lipid metabolites in spermatozoa across three compartments. Int J Mol Sci 2022;23(19).

